7718 *Macromolecules* **2009**, *42*, 7718–7735
DOI: 10.1021/ma901657n

Macromolecules
ARTICLE

Examination of the Thermal and Thermomechanical Behavior of Novel Cyanate Ester Homopolymers and Blends with Low Coefficients of Thermal Expansion

Ian Hamerton,*,† Brendan J. Howlin,† Paul Klewpatinond,† and Shinji Takeda‡

†*Chemical Sciences Division, Faculty of Health and Molecular Sciences, University of Surrey, Guildford, Surrey GU2 7XH, United Kingdom, and* ‡*Advanced Materials Research & Development Centre, Hitachi Chemical Co. Ltd., 1500 Ogawa, Chikusei, Ibaraki 317-8555, Japan*

Received June 12, 2009; Revised Manuscript Received September 10, 2009

ABSTRACT: A new four-step synthetic method is presented and applied to the preparation in high purity of three novel dicyanate monomers that comprise aryl/alkylene ether backbones with high molecular flexibility. The multistep route involves four individually high-yielding steps (each ≥70%), thus giving overall reaction yields for total synthesis of 42−50% depending on the length of the backbone. All products are characterized using FT-IR and ^{1}H NMR spectroscopy, elemental analysis, and melting point determination. DSC analysis of "uncatalyzed" samples displays relatively sharp melting endotherms ranging from 66 to 125 °C depending on the length (i.e., flexibility) of the backbone. All monomers display broad polymerization exothe rms (87 ± 2 kJ/mol cyanate), although the polymerizations occur in different temperature regimes. When catalyzed (aluminum(III) acetylacetonate/dodecylphenol), the exothermic polymerization peaks occur at significantly lower temperatures than the uncatalyzed analogues and have much narrower profiles but tend to occur in a similar temperature regime (i.e., peak maxima 205−216 °C). The polymerization enthalpies for the catalyzed monomers are ca. 93 ± 9.9 kJ/mol cyanate. TGA shows that the polymers typically lose 5% of their masses by ca. 346−366 °C, which is comparable to AroCy B10. DMTA analysis of cured AroCy B10 yields results that are consistent with published data, and T_g values (tan δ_{max}) of the homopolymers are 221 (**4a**), 139 (**4b**), and 121 °C (**4c**) and fall with increasing backbone length/flexibility. The storage moduli at 25 °C for the binary blends are significantly lower than the respective homopolymers, but the reduction in E' (25−200 °C) is significantly improved compared with AroCy B10. When combined with AroCy B10 in binary blends, the new monomers showed a reduction in CTE of up to 12 ppm/°C while maintaining the same value of T_g.

Introduction

The commercial introduction of a prepolymer of bisphenol A dicyanate in 1975[1] was initially targeted at the then new and growing market for substrates for advanced printed circuit boards. The combination of exceptionally low dielectric constants, ε = 2.2 to 2.7, and dissipation factors, D_f = 0.003, at gigahertz frequencies coupled to low loss behavior has ensured the continuing application of cyanates in the fabrication of microelectronics components such as multichip modules (MCMs)[2] and latterly in stealthy coatings and structures.[3] Cured cyanates typically offer high-performance characteristics somewhat intermediate between epoxy resins and bismaleimide (BMI)[4] (e.g., glass-transition temperatures, T_g, of between 200 and 300 °C depending on structure and degree of cure) although very low moisture absorption (as low as 0.6 to 2.5 wt % depending on backbone structure, compared with figures of 4 to 4.5 wt % for BMIs or 3−6 wt % for commercial epoxies). This can lead to good hot/wet properties; for example, when cured, the methylated commercial monomer AroCy M was found to retain 83% of its flexural modulus at 150 °C after immersion in boiling water, compared with 53% for a commercial aerospace epoxy (based on a tetraglycidyl amine),[5] and thus cyanates have been used as advanced structural composite matrices. In this application, the composite materials may be formulated to achieve attractive levels of fracture toughness (e.g., G_{IC} = 454 J/m^2 for Fiberite 954-3) for thermoset polymers after blending with engineering thermoplastics.[6]

Cyanates may adhere to a variety of substrates; for example, metals, glass and carbon fibers, and cyanate adhesives have yielded values of 14−20 MPa (for lap shear strength) on 20224 T-3 aluminum alloy (some 50−100% higher than corresponding aerospace epoxy adhesives (cured with aromatic diamines)), but it is their behavior on silicon that is of particular interest in the microelectronics arena because of the ubiquity of this material in the formation of MCMs. Typically, the latter are formed from sequentially built layers of metallized conductors on ceramic or silicon substrates and unreinforced polymer dielectric films. Despite (and partially owing to) the good adhesion observed on these substrates, there remains the strong possibility of disbonding and delamination of the layers as thermal processing takes place, given the large differences in the coefficients of thermal expansion (CTE) of the components used in MCMs. Inevitably, with a complex structure of this kind, the costs mount as the likelihood of scrapping a multilayer board increases with layer count. The aim of the present work was stimulated by the drive to produce polymers with relatively high T_g values but combined with superior fracture toughness with lower values of CTE than those currently observed in commercial resin systems.

This necessitated a different synthetic approach: a number of preparative routes to cyanate monomers have been reported and reviewed comprehensively,[7] although the most important

*To whom correspondence should be addressed: E-mail: i.hamerton@surrey.ac.uk.

 Published on Web 09/30/2009

commercial route, first reported by Grigat and Pütter some 40 years ago[8,9] and involving the treatment of phenols with cyanogen chloride (or more typically cyanogen bromide in laboratory preparations such as the route reported in this work), still form the basis of modern methods, albeit in a modified form. Importantly, although the preparation involves the use of toxic reagents, the resulting monomers generally have low toxicities (e.g., $LD_{50} \geq 3$ g/kg for the dicyanate of bisphenol A). In previous unreported experiments[10] designed to produce the dicyanates examined within this article, the use of a variety of protecting groups (e.g., tetrahydropyranyl, benzyl or methyl ethers, etc.) met with limited success. For example, having produced (*bis*-4-(4-methoxyphenoxy) phenylethoxyethane from dichloroethane in high yield and purity (with the intention of cleaving the methyl ether to yield the diphenol prior to cyanation), it was not possible to deprotect this group using, for example, recognized methods such as boron tribromide[11] without breaking the alkylene ether backbone. Consequently, it was decided that it would be better to find a new protecting group and use a suitable aldehyde as a protecting group to enable its removal easily while leaving the alkylene ether backbone intact, and this led to the current study.

Experimental Section

Materials. The following reagents were obtained from a range of sources and were all used as received, unless otherwise noted in the experimental text. Dichloromethane (DCM), methanol, acetone, *N*,*N*-dimethylformamide (DMF), anhydrous potassium carbonate, phosphorus pentoxide, sodium thiosulphate, sodium hydrogen carbonate, sodium sulfate, sodium hydroxide (all GPR grade and obtained from Fisher Scientific). *N*,*N*-Dimethylacetamide (DMAc) (99%), triethylamine (99%), deuteriated solvents ($CDCl_3$, CD_6CO, CD_3OD), dichloroethane, 2-chloroethylether, 1,2-*bis*-(2-chloroethoxy)ethane, 4-hydroxybenzaldehyde, and 3-chloroperoxybenzoic acid (70−75%) were all obtained from Aldrich Chemical. 4-Methoxyphenol (99%) was obtained from Acros Organics and anhydrous sodium sulfate (GPR) was obtained from BDH Chemicals. The commercial dicyanate monomer, AroCy B10, based on bisphenol A was obtained from Ciba Specialty Chemicals. Aluminum(III) acetylacetonate ($Al(acac)_3$) (99%) and 4-dodecylphenol (mixture of isomers) were obtained from Sigma Aldrich.

Apparatus. Fourier transform infrared (FT-IR) spectra were recorded using a Perkin-Elmer (system 2000 FT-IR) spectrometer interfaced with a PC running PE-Spectrum v 2.00 software or a Nicolet Avatar 320 FT-IR spectrometer running Nicolet OMNIC ESP 5.1 software. The samples were presented on an ATR module; 16 scans, at a resolution of 4 cm^{-1}, were recorded and coadded to produce the final spectrum. ^1H nuclear magnetic resonance (NMR) spectra were obtained using a Bruker AC300 spectrometer operating at 300 MHz. Solutions of samples were prepared in $CDCl_3$, CD_3OD, and acetone-d_6 according to solubility, and spectra were acquired at 298 K using tetramethylsilane (TMS) as an internal standard where applicable.

Elemental analysis (samples 1−3 mg) was performed using a Leeman Laboratories CE 440 elemental analyzer. Acetanilide was used to calibrate the instrument, followed by a set of standards (*S*-benzyl thiuronium chloride and phenylthoiurea). The accuracy with standard organic compounds is ±0.15% absolute plus ±0.15% relative. Melting temperatures were determined using a Kopfler flat bed micro melting point (mp) apparatus and a heating rate of 4 K min^{-1}.

Differential scanning calorimetry (DSC) experiments were performed using a TA Instruments DSC Q100 series controlled by a Viglen computer running TA Q series advantage software. Samples (ca. 4.5 ± 0.5 mg) were encapsulated in crimped aluminum pans and placed in the heating chamber at ca. 25 °C and heated rapidly to 40 °C and held for 1 min to equilibrate before data recording began. All measurements were made under N_2 (flow rate of 20 cm^3 min^{-1}) at a variety of heating rates (5, 10, 15, and 20 K min^{-1}) over the temperature range 35−350 °C. For T_g measurements, following the initial 10 K min^{-1} scan, samples were quenched and cooled at the same rate prior to a second rescan experiment at 10 K min^{-1}. We determined the T_g by measuring the midpoint position of the discontinuity of the baseline.

Thermogravimetric (TG) analysis was performed using a ULVAC Sinku-Riko differential thermogravimetric analyzer TGD 7000. Prior to running the sample, the sample holder (platinum boat) was heated (80 K min^{-1}) to over 800 °C to remove any residual material from any previous experiments, and allowed to cool to room temperature. The shaved samples (ca. 8.7 ± 0.5 mg) of the cured neat resin were measured (under N_2, 20 cm^3 min^{-1}) at a heating rate of 10 K min^{-1} between 25 and 800 °C.

Dynamic mechanical thermal analysis (DMTA) measurements were undertaken in dual cantilever bending mode on cured neat resin and blend samples (10 × 30 × 1 mm^3) using a Polymer Laboratories dynamic mechanical thermal analyzer with a Polymer Laboratories environmental controller unit. Temperature scans were performed between −150 and 300 °C at 5 K min^{-1} at a frequency of 1 Hz.

Thermomechanical analysis (TMA) measurements were undertaken using a Seiko Instruments EXSTAR6000 TMA/SS6000 apparatus and calibrated using quartz crystal with a known CTE, before measurements were performed in penetration mode (probe weight 4.9 mN, analysis surface area 9.026 mm^2) on cured neat resin samples (ca. 0−7−1.1 × 5 × 5 mm^3) supported on quartz. Temperature scans were performed between 25 and 300 °C at 5 K min^{-1}.

Synthesis and Characterization. Several general methods were combined to produce three different cyanate ester monomers, differing only in the bridging chain length (i.e., the value of *n*). Consequently, the entire preparative procedure is described for compounds **1a**, **2a**, **3a**, and **4a** ($n = 1$), but for the remaining compounds, only the quantities of the reagents, the characterization data, and variations in the method are given.

Preparation of 4,4′-[Ethane-1,2-diylbis(oxy)]dibenzaldehyde (1a, $n = 1$). A three-necked round-bottomed flask, equipped with a magnetic stirrer bar, thermometer, and condenser was charged with 4-hydroxybenzaldehyde (153.62 g, 1.26 mol), dichloroethane (62.24 g, 0.63 mol), K_2CO_3 (347.72 g, 2.52 mol), and DMF (500 cm^3). The mixture was stirred and heated to reflux (110 °C, 48 h) under a nitrogen blanket. The reaction mixture was left to cool to room temperature before extracting into DCM; then, water was added to dissolve any salts. The DCM product layer was removed, and the aqueous layer was washed with DCM. The DCM layers were combined and washed with water and dried over sodium sulfate (room temperature, overnight). The solvent was removed by rotary evaporation and under reduced pressure to obtain a crude product. A needlelike, off-white crystalline solid was obtained by recrystallization in warm diethyl ether, and the product was collected by filtration and dried in a desiccator with P_2O_5 under reduced pressure (overnight) to yield 124.06 g (72.9%). mp 113−115 °C. Anal. Calcd for $C_{16}H_{14}O_4$: C, 71.10; H, 5.22. Found: C, 70.59; H, 4.75. ^1H NMR (300 MHz, $CDCl_3$, δ_H, from TMS): 9.91 (1H, s, C−H due to aldehyde), 7.88−7.85 (4H, d, $J_H = 8.8$ Hz, Ar−H ortho to aldehyde link), 7.08−7.05 (4H, d, $J_H = 8.8$ Hz, Ar−H and meta to aldehyde link), 4.45 (4H, s, C−H between ether links para to aldehyde links).

Preparation of 4,4′-[Ethane-1,2-diylbis(oxy-1,4-phenylene)]-diformate (2a, $n = 1$). A three-necked round-bottomed flask, equipped with a magnetic stirrer bar, thermometer, and condenser was charged with *bis*-(4,4′-formylphenoxy)ethane (120.71 g, 0.45 mol), 3-chloroperoxybenzoic acid (300.63 g, 1.74 mol added portionwise), and DCM (900 cm^3). *Caution should be taken, and the reagent, particularly in these quantities, should be added portionwise with stirring because the reaction is*

strongly exothermic. The mixture was stirred at room temperature (4 h) under a nitrogen blanket. A milky suspension was formed, and the resultant reaction mixture was treated with saturated (aq) $NaHCO_3$ (600 cm^3). After ca. 2 h, and when the mixture had stopped effervescing, the DCM layer was collected, and the aqueous layer was washed with DCM (3 × 50 cm^3). The organic layers were combined and washed with 10% $Na_2S_2O_3$ (aq) (3 × 50 cm^3), followed by water (3 × 50 cm^3) and brine (3 × 50 cm^3), and finally dried over sodium sulfate (overnight). The solvent was removed by rotary evaporation under reduced pressure to obtain a crude product. A white crystalline solid was obtained by recrystallization from warm methanol, and the product was collected by filtration and dried in a desiccator with P_2O_5 under reduced pressure to yield 109.39 g (81.0%). mp 133−135 °C. Anal. Calcd for $C_{16}H_{14}O_6$: C, 63.57; H, 4.67. Found: C, 63.41; H, 4.56. ^{1}H NMR (300 MHz, $CDCl_3$, δ_H, from TMS): 8.28 (1H, s, C−H due to oxy aldehyde), 7.08−7.05 (4H, d, J_H = 8.8 Hz, Ar−H ortho to oxy aldehyde link), 6.97−6.94 (4H, d, J_H = 9.3 Hz, Ar−H and meta to oxy aldehyde links), 4.31 (4H, s, C−H between ether links para to oxy aldehyde links).

Preparation of 4,4′-[Ethane-1,2-diylbis(oxy)]diphenol (3a, *n* = 1). A three-necked round-bottomed flask, equipped with a magnetic stirrer bar, thermometer, and condenser was charged with *bis*-(4,4′-formyloxyphenoxy)ethane (108.02 g, 0.36 mol), sodium hydroxide (57.18 g, 1.43 mol), ethanol (800 cm^3), and water (300 cm^3). The mixture was stirred and heated to reflux (130 °C, 24 h) under a nitrogen blanket. The reaction mixture was left to cool to room temperature before neutralizing with hydrochloric acid (3 M), forming a solid that was extracted into DCM. The DCM layers were combined and washed with water and dried over sodium sulfate; the solvent was removed by rotary evaporation under reduced pressure to obtain a crude product. A solid was obtained by recrystallization in warm ethanol and water; then, the product was collected by filtration and dried in a desiccator with P_2O_5 under reduced pressure to yield 70.25 g (79.8%). mp 213−215 °C. Anal. Calcd for $C_{14}H_{14}O_4$: C, 68.28; H, 5.73. Found: C, 67.90; H, 5.69. ^{1}H NMR (300 MHz, CD_3OD, δ_H, from TMS): 6.82−6.79 (4H, d, J_H = 8.8 Hz, Ar−H ortho to hydroxy link), 6.72−6.69 (4H, d, J_H = 8.8 Hz, Ar−H and meta to hydroxy links), 4.18 (4H, s, C−H between ether links para to hydroxy links).

Preparation of 4,4′-[Ethane-1,2-diylbis(oxy-1,4-phenylene)]dicyanate (4a, *n* = 1). A three-necked round-bottomed flask, equipped with a magnetic stirrer bar, a dropping funnel, and a drying tube, was charged with *bis*-(4,4′-hydroxyphenoxy)ethane (69.82 g, 0.28 mol) and cyanogen bromide (66.07 g, 0.62 mol). The reactants were dissolved in acetone (800 cm^3), and the solution was cooled to below −5 °C in a methanol/cardice bath. Triethylamine (63.18 g, 0.62 mol) was added dropwise via the dropping funnel to the stirring solution at a rate such that the reaction mixture was maintained below −5 °C. After the addition of triethylamine, the reaction mixture was left stirring for 30 min and then allowed to warm to room temperature. The mixture was washed by fast stirring with water to remove triethylamine hydrobromide (the principal byproduct). The product was extracted with DCM and washed with water (3 × 50 cm^3). The organic product layer was dried over sodium sulfate, and the solvent was removed by rotary evaporation to give the crude product. A light-yellow solid was obtained by recrystallization from a 50/50 mixture of ethanol and water to yield 79.02 g (94.1%). mp 118−120 °C. Anal. Calcd for $C_{16}H_{12}N_2O_6$: C, 64.86; H, 4.08; N, 9.46. Found: C, 64.49; H, 3.81; N, 9.27. ^{1}H NMR (300 MHz, $CDCl_3$, δ_H, from TMS): 7.26−7.23 (4H, d, J_H = 9.3 Hz, Ar−H ortho to cyanate link), 7.02−6.97 (4H, d, J_H = 9.3 Hz, Ar−H and meta to cyanate links), 4.33 (4H, s, C−H between ether links para to cyanate links).

Preparation of 4,4′-[Oxybis(ethane-1,2-diyloxy)]dibenzaldehyde (1b, *n* = 2). Using the previous method, the following quantities were used: 4-hydroxybenzaldehyde (77.70 g, 0.64 mol), dichloroethane (45.5 g, 0.32 mol), potassium carbonate (175.88 g, 1.27 mol), and DMF (400 cm^3). A light-yellow crystalline solid was obtained by recrystallization from warm diethyl ether. Yield: 90.25 g (90.3%). mp 130−132 °C. Anal. Calcd for $C_{18}H_{18}O_5$: C, 68.78; H, 5.77. Found: C, 67.64; H, 5.70. ^{1}H NMR (300 MHz, $CDCl_3$, δ_H, from TMS): 9.89 (1H, s, C−H due to aldehyde), 7.84−7.81 (4H, d, J_H = 8.8 Hz, Ar−H ortho to aldehyde link), 7.03−7.00 (4H, d, J_H = 8.8 Hz, Ar−H and meta to aldehyde link), 4.26−4.23 (4H, t, J_H = 4.5 Hz, C−H between ether links para to aldehyde links), 3.99−3.96 (4H, t, J_H = 4.5 Hz, C−H between ether links in the center of the molecule).

Preparation of 4,4′-[Oxybis(ethane-1,2-diyloxy-1,4-phenylene)]diformate (2b, *n* = 2). Using the previous method, the following quantities were used: *bis*-(4,4′-formylphenoxy)ethoxyethane (88.94 g, 0.28 mol), 3-chloroperoxybenzoic acid (190.47 g, 1.10 mol), DCM (800 cm^3), and saturated (aq) $NaHCO_3$ (500 cm^3). A light-yellow crystalline solid was obtained by recrystallization from warm methanol. Yield: 80.84 g (82.5%). mp 67−69 °C. Anal. Calcd for $C_{18}H_{18}O_7$: C, 62.42; H, 5.24. Found: C, 62.10; H, 5.10. ^{1}H NMR (300 MHz, $CDCl_3$, δ_H, from TMS): 8.28 (1H, s, C−H due to oxy aldehyde), 7.06−7.03 (4H, d, J_H = 9.3 Hz, Ar−H ortho to oxy aldehyde link), 6.94−6.91 (4H, d, J_H = 9.3 Hz, Ar−H and meta to oxy aldehyde links), 4.16−4.13 (4H, t, J_H = 4.5 Hz, C−H between ether links para to oxy aldehyde links), 3.94−3.91 (4H, t, J_H = 4.5 Hz, C−H between ether links in the center of the molecule).

Preparation of 4,4′-[Oxybis(ethane-1,2-diyloxy-1,4-phenylene)]diphenol (3b, *n* = 2). Using the previous method, the following quantities were used: *bis*-(4,4′-formyloxyphenoxy)ethoxyethane (79.93 g, 0.23 mol), sodium hydroxide (36.92 g, 0.92 mol), ethanol (600 cm^3), and water (200 cm^3). A light-brown solid was obtained by recrystallization in warm ethanol and water. Yield: 45.18 g (67.4%). mp 95−97 °C. Anal. Calcd for $C_{16}H_{18}O_5$: C, 66.19; H, 6.25. Found: C, 65.78; H, 6.41. ^{1}H NMR (300 MHz, CD_3OD, δ_H, from TMS): 6.80−6.77 (4H, d, J_H = 8.9 Hz, Ar−H ortho to hydroxy link), 6.70−6.67 (4H, d, J_H = 8.9 Hz, Ar−H and meta to hydroxy links), 4.07−4.04 (4H, t, J_H = 4.5 Hz, C−H between ether links closest to Ar−O para to hydroxy links), 3.86−3.83 (4H, t, J_H = 4.5 Hz, C−H between ether links in the center of the molecule).

Preparation of 4,4′-[Oxybis(ethane-1,2-diyloxy-1,4-phenylene)]dicyanate (4b, *n* = 2). Using the previous method, the following quantities were used: *bis*-(4,4′-hydroxyphenoxy)ethoxyethane (44.36 g, 0.16 mol), cyanogen bromide (36.98 g, 0.35 mol), acetone (800 cm^3), and triethylamine (35.44 g, 0.35 mol). An off-white solid was obtained by recrystallization from a 50/50 mixture of ethanol and water to yield 47.78 g (97.9%). mp 109−111 °C. Anal. Calcd for $C_{18}H_{16}N_2O_5$: C, 63.52; H, 4.74; N, 8.23. Found: C, 63.09; H, 4.63; N, 7.99. ^{1}H NMR (300 MHz,$CDCl_3$, δ_H, from TMS): 7.23−7.18 (4H, m, J_H = 9.3 Hz, Ar−H ortho to cyanate link), 6.98−6.93 (4H, m, J_H = 9.3 Hz, Ar−H and meta to cyanate links), 4.17−4.13 (4H, t, J_H = 4.5 Hz, C−H between ether links closest to Ar−O para to cyanate links), 3.94−3.91 (4H, t, J_H = 4.5 Hz, C−H between ether links in the center of the molecule).

Preparation of 4,4′-[Ethane-1,2-diylbis(oxyethane-1,2-diyloxy-1,4-phenylene)]dibenzaldehyde (1c, *n* = 3). Using the previous method, the following quantities were used: 4-hydroxybenzaldehyde (68.15 g, 0.56 mol), dichloroethane (52.20 g, 0.28 mol), potassium carbonate (154.26 g, 1.12 mol), and DMF (400 cm^3). A very light-brown crystalline solid was obtained by recrystallization in warm diethyl ether. Yield: 85.89 g (85.9%). mp 63−65 °C. Anal. Calcd for $C_{20}H_{22}O_6$: C, 67.03; H, 6.19. Found: C, 65.87; H, 6.14. ^{1}H NMR (300 MHz, $CDCl_3$, δ_H, from TMS): 9.88 (1H, s, C−H due to aldehyde), 7.84−7.81 (4H, d, J_H = 8.8, Ar−H ortho to aldehyde link), 7.02−7.00 (4H, d, J_H = 8.2, Ar−H and meta to aldehyde link), 4.23−4.19 (4H, t, J_H = 4.5, C−H between ether links para to aldehyde links), 3.91−3.88 (4H, t, J_H = 4.5, C−H between ether links closest to Ar−O−CH_2), 3.76 (4H, s, C−H at center of the molecule).

Preparation of 4,4′-[Ethane-1,2-diylbis(oxyethane-1,2-diyloxy-1,4-phenylene)]diformate (2c, *n* = 3). Using the previous method,

the following quantities were used: *bis*-(4,4′-formylphenoxy)-ethoxyethane (82.62 g, 0.23 mol), 3-chloroperoxybenzoic acid (155.19 g, 0.90 mol), DCM (800 cm^3), and saturated (aq) $NaHCO_3$ (500 cm^3). An off-white solid was obtained by recrystallization from methanol. Yield: 70.09 g (77.9%). mp 34−36 °C. Anal. Calcd for $C_{20}H_{22}O_8$: C, 61.53; H, 5.68. Found: C, 60.72; H, 5.76. ^{1}H NMR (300 MHz, $CDCl_3$, δ_H, from TMS): 8.27 (1H, s, C−H due to oxy aldehyde), 7.05−7.02 (4H, d, J_H = 9.3, Ar−H ortho to oxy aldehyde link), 6.93−6.90 (4H, d, J_H = 8.8, Ar−H and meta to oxy aldehyde links), 4.13−4.10 (4H, t, J_H = 4.5, C−H between ether links para to oxy aldehyde link), 3.88−3.86 (4H, t, J_H = 4.5, C−H between ether links closest to Ar−O−CH_2), 3.75 (4H, s, C−H at center of the molecule).

Preparation of 4,4′-[Ethane-1,2-diylbis(oxyethane-1,2-diyloxy-1,4-phenylene)]diphenol (3c, *n* = 3). Using the previous method, the following quantities were used: *bis*-(4,4′-formyloxyphenoxy)ethoxyethane (68.89 g, 0.18 mol), sodium hydroxide (28.23 g, 0.71 mol), ethanol (75 cm^3), and water (25 cm^3). A light-yellow needlelike crystalline solid was obtained by recrystallization from warm ethanol and water. Yield: 50.27 g (85.2%). mp 108−110 °C. Anal. Calcd for $C_{18}H_{22}O_6$: C, 64.66; H, 6.63. Found: C, 64.41; H, 6.84). ^{1}H NMR (300 MHz, CD_3OD, δ_H, from TMS): 6.79−6.76 (4H, d, J_H = 9.3, Ar−H ortho to hydroxy link), 6.71−6.67 (4H, d, J_H = 8.8, Ar−H and meta to hydroxy links), 4.04−4.00 (4H, t, J_H = 4.5, C−H between ether links closest to Ar−O para to hydroxy link), 3.80−3.77 (4H, t, J_H = 4.5, C−H between ether links closest to Ar−O−CH_2), 3.70 (4H, s, C−H at center of the molecule).

Preparation of 4,4′-[Ethane-1,2-diylbis(oxyethane-1,2-diyloxy-1,4-phenylene)]dicyanate (4c, *n* = 3). Using the previous method, the following quantities were used: *bis*-(4,4′-hydroxyphenoxy)-ethoxyethane (49.58 g, 0.15 mol), cyanogen bromide (34.56 g, 0.33 mol), acetone (500 cm^3), and triethylamine (33.05 g, 0.33 mol). We obtained an off-white solid by adding a 50/50 mixture of ethanol and water. Yield: 50.27 g (85.2%). mp 108−110 °C. Anal. Calcd for $C_{20}H_{20}N_2O_6$: C, 62.49; H, 5.24; N, 7.28. Found: C, 62.41; H, 5.15; N, 7.18. ^{1}H NMR (300 MHz, $CDCl_3$, δ_H, from TMS): 7.22−7.19 (4H, m, J_H = 9.3, Ar−H ortho to cyanate link), 6.96−6.93 (4H, m, J_H = 9.3, Ar−H and meta to cyanate links), 4.14−4.11 (4H, t, J_H = 4.5, C−H between ether links closest to Ar−O para to cyanate link), 3.88−3.85 (4H, t, J_H = 4.5, C−H between ether links closest to Ar−O−CH_2), 3.75 (4H, s, C−H at center of the molecule).

Formulation of Monomer/Cocatalyst Blends. Time constraints precluded the preparation of a full series of binary blends to determine the optimum blend composition, and so the level of 20 wt % was chosen (based on previous published work involving toughening agents) for all blends. Prior to incorporation in the dicyanate, the cocatalyst package, comprising $Al(acac)_3$ and dodecylphenol in the molar ratio of 1:25, was first homogenized by heating to 80 °C (in a vial in a water bath) before cooling to room temperature. The cocatalysts were then introduced into the dicyanate monomers by mixing in a pestle and mortar at room temperature to a homogeneous mixture. (See Table 1 for molar ratios.) Thermal analyses were performed directly after blending, but storage of catalyzed blends was undertaken in a refrigerator (+5 °C) with care being taken to minimize the exposure of the blends to atmospheric moisture.

Results and Discussion

The original choice for an examination of the alkylene ether backbone moiety was prompted by previous work by one of the coauthors,[12] albeit with BMIs for which brittleness can also be a challenge. However, in this previous publication, the synthetic route employed for the preparation of BMIs via diamines, followed by cyclodehydration of the corresponding bismaleamic acid, could not be employed directly with the present compounds, necessitating a different approach. During the current work, a series of three cyanate monomers having similar alkylene ether backbone structures that differ in length and are generically identified by n = 1, 2, 3 to denote the number of ethoxy segments in the chain (**4a**,**b**,**c**) was successfully prepared in good yield by the same four-step reaction pathway (Scheme 1) using aldehydic protecting groups. The first step was a modified combination of reported methods of ether synthesis of hydroxyaldehydes previously reported by different authors: for example, Jiang et al.[13] prepared the dialdehyde n = 1 (**1a**) by reacting dibromoethane and 4-hydroxybenzaldehyde with LiH as the reducing agent at −78 °C in ethanol over 2.5 days. A similar reaction was carried out by Simion et al.[14] using a 2% NaOH solution as the reducing agent and refluxed in ethanol for 72 h and then over ice for a further 24 h. Similarly, the dialdehyde n = 3 (**3a**) was synthesized by Guilani et al.[15] using Na metal dissolved in ethanol and refluxed overnight. The second and third steps of the procedure were modified from that reported by Nagvekar et al.[16] involving the conversion of terminal aldehyde to hydroxyl via oxyaldehydic functions. Reactions for the synthesis of the dicyanate monomers (**4a**,**b**,**c**) were subsequently scaled up first from 10 to 40 g and then to 100 g preparations; all scale-up reactions gave comparable results to those of the initial reactions. For the purpose of this

Table 1. Catalyst and Monomer Molar Ratios

	molar ratio		
monomer	$Al(acac)_3$	dodecylphenol	monomer(s)
AroCy B10	1	25	1000
4a	1	25	2000
4b	1	25	2000
4c	1	25	2000
AroCy B10−**4a**	1	25	2000
AroCy B10−**4b**	1	25	2000
AroCy B10−**4c**	1	25	2000

Scheme 1. Synthetic Route to the Dicyanate Monomers (4a, 4b, 4c).

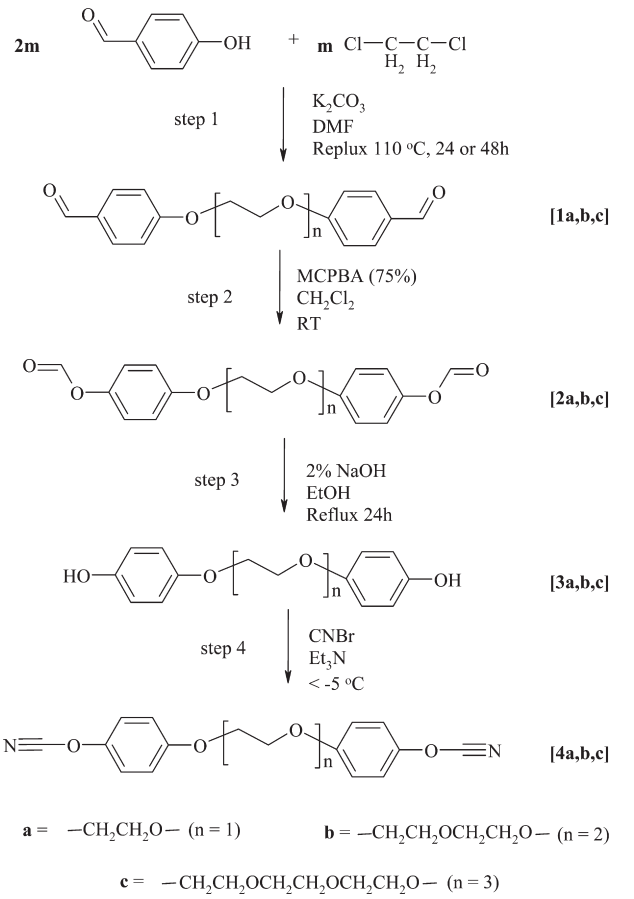

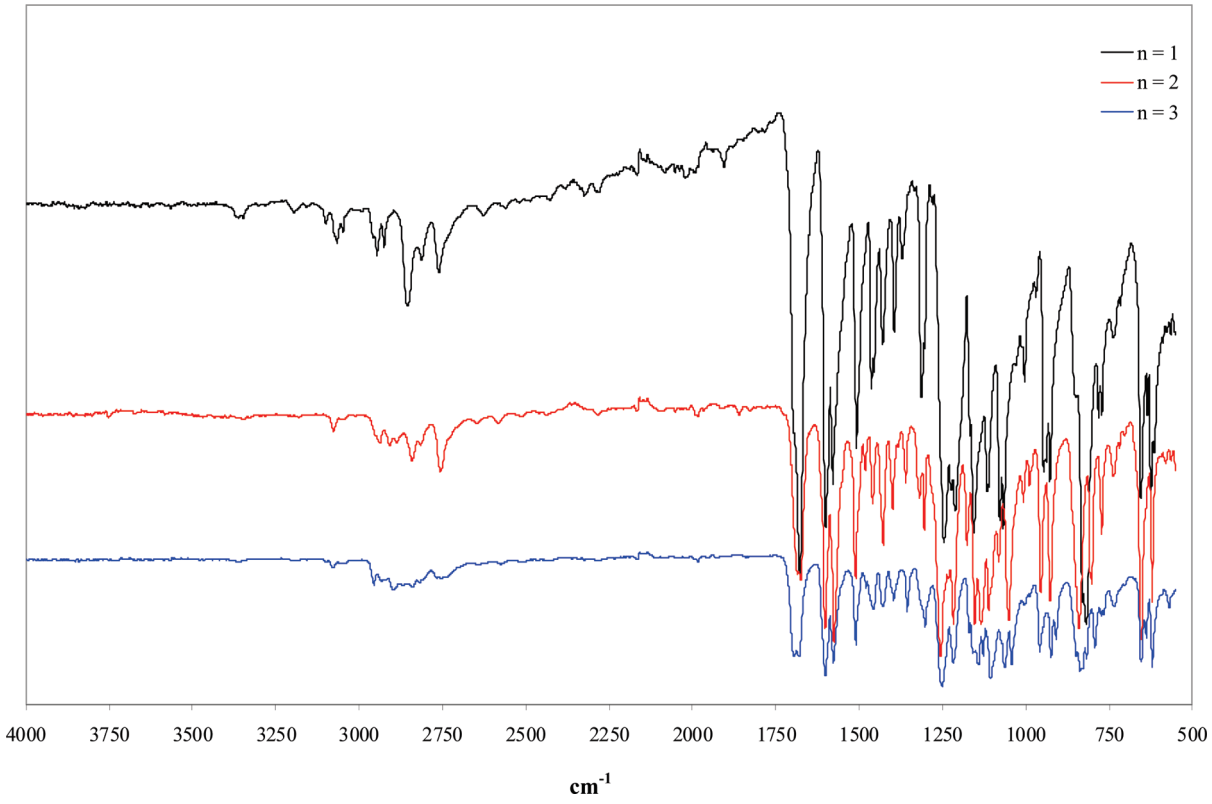

Figure 1. Infrared transmission spectra of the dialdehydes produced in step 1 (common arbitrary vertical scale).

Table 2. FT-IR Assignments for the Dialdehydes from Step 1

	compounds/observed bands (cm^{-1})		
assignment	**1a**	**2a**	**3a**
Ar−H stretch	3066	3078	3079
$-CH_2-$ stretch (ethoxy)	2946−2925	2938−2886	2956−2899
−C−H stretch (aldehyde)	2855−2760	2842	2839−2751
ring skeleton	1600−1507	1601−1510	1600−1509
aliphatic CH_2 scissor	1463−1455	1481−1459	1478−1457
first overtone aldehydic C−H bending vibrations	1394	1399	1395
Ar−O−R (asymmetric)	1244−1211	1255−1216	1250−1216
Ar−O−R (symmetric)	1155−1066	1153−1080	1158−1042
1,4-disubstituted benzene ring (out-of-plane bending)	829−818	840	836

study, the analyses of the final scale-up preparations of the three dicyanates were used for the polymer preparations and are discussed below. This first preparative step was common for all three backbones, differing only slightly in terms of reaction time and reaction workup method, and the infrared spectra are shown (Figure 1) for all dibenzaldehydes (**1a**,**b**,**c**). For characterization purposes, the principal peaks of interest (Table 2) are those produced by the aldehyde. (Two aldehydic C−H stretching bands at ca. 2800 cm^{-1} produce the first overtone at ∼1390 cm^{-1} and are accompanied by a strong carbonyl stretching band at ∼1670 cm^{-1}). The ether backbone structures, for example, the CH_2 stretching bands for the alkyl ether backbone, appear at 2900 cm^{-1}, along with the aryl−alkyl ether stretching at around 1200 (asymmetric stretch) and 1100 cm^{-1} (symmetric stretch), respectively, and tended to remain largely unchanged throughout the entire preparation).

This is good evidence of the presence of the aldehyde group, especially when the first overtone does not shift significantly from 1390 cm^{-1}. ^{1}H NMR spectroscopy was also employed to verify the presence of the respective structures, and a representative spectrum for **1a** is shown in Figure 2.

The ^{1}H NMR spectrum of **1a** (Figure 2) reveals that whereas the reaction was generally successful in producing a relatively clean product, a small amount of workup DCM residue was revealed at 5.27 ppm (as evidenced by the poorer agreement of the elemental analysis). In the ^{1}H NMR spectrum of product **1b**, the methylene groups are now nonequivalent, and the effects of the electronegativity of the oxygen atoms on either side of the backbone are reduced (because of the electropositive methylene from the aliphatic ether link), moving the triplet [of H_a] downfield from 4.45 to 4.26 to 4.23 ppm. Compared with **1a**, there is now only one oxygen atom deshielding the aliphatic ether methylenes, and thus the triplet moves upfield to 3.99 to 3.96 ppm. A similar situation was revealed with the ^{1}H NMR spectrum of product (**1c**) with a small amount of workup DCM residue at 5.27 ppm and the clearly attributable shifts because of the methylene protons in the nonequivalent positions.

In the second step, the bands of interest are associated with the formate group (Figure 3) as the CH_2 stretching bands for the alkyl ether backbone were very similar to products of the previous step (and indeed in later steps offering little discrimination). As expected, the two aldehydic C−H stretching bands (ca. 2800 cm^{-1} in Figure 1) are now absent from the spectra, and the carbonyl stretching band is now observed at ∼1700 cm^{-1} for the formates and is accompanied by a "C−O" stretch, a combination band) at ca. 1280 cm^{-1} (Table 3).

A representative ^{1}H NMR spectrum for the diformate (**2b**) produced in step 3 is shown in Figure 4. For **2a**, the inductive and anisotropic effects of C═O appear to have a minimal affect on the ring protons, although the introduction of the oxygen para to the ethereal oxygen has increased the electronegativity on the ring protons, causing them to move upfield 7.08 to 7.05 ppm and 6.97 to 6.94 ppm relative to shifts for unsubstituted benzene at 7.27 ppm. Calculated substituent effects for −OH on a 1,4-disubstituted benzene place the signal upfield by a ca. 0.2 ppm.

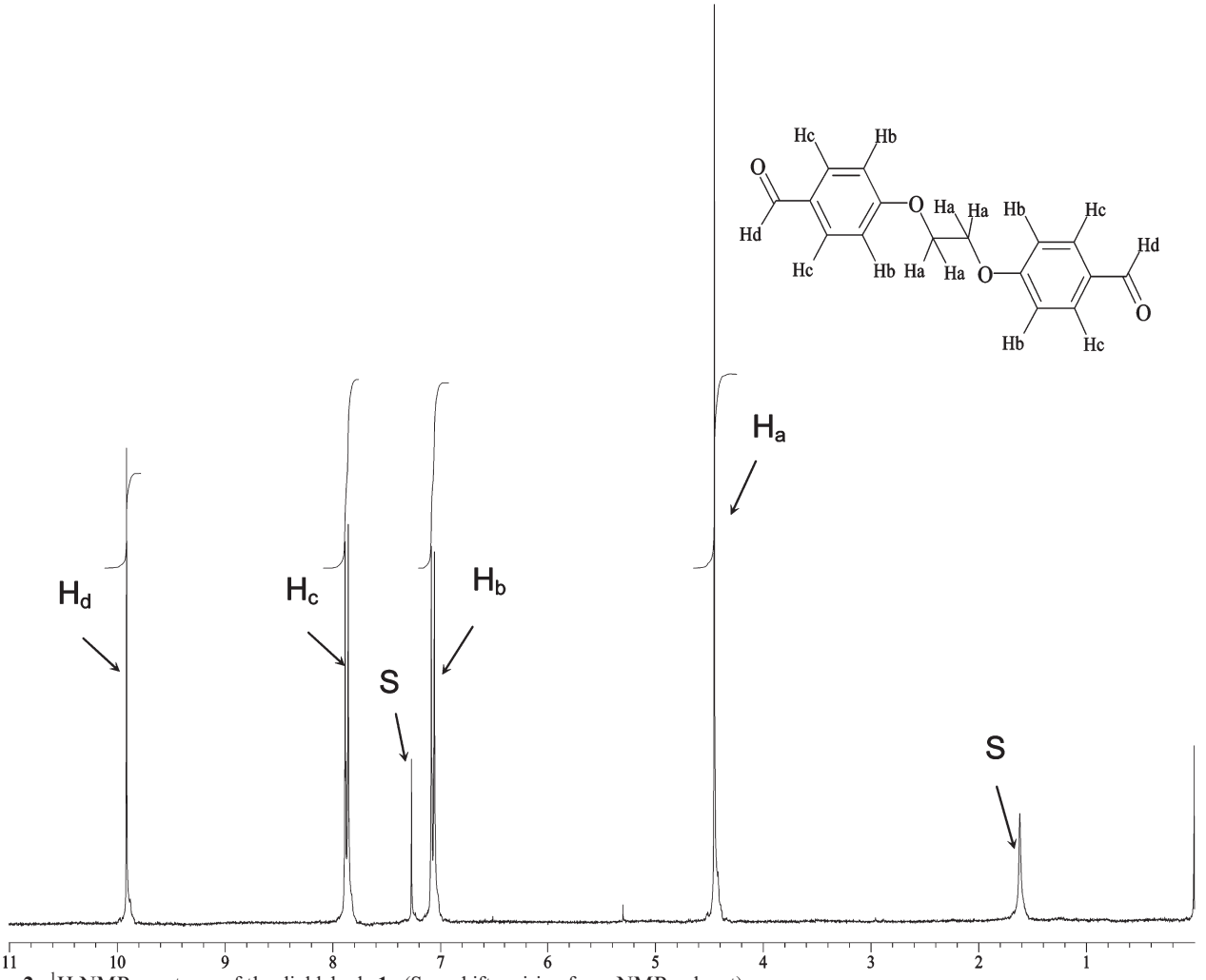

Figure 2. ^{1}H NMR spectrum of the dialdehyde **1a** (S = shifts arising from NMR solvent).

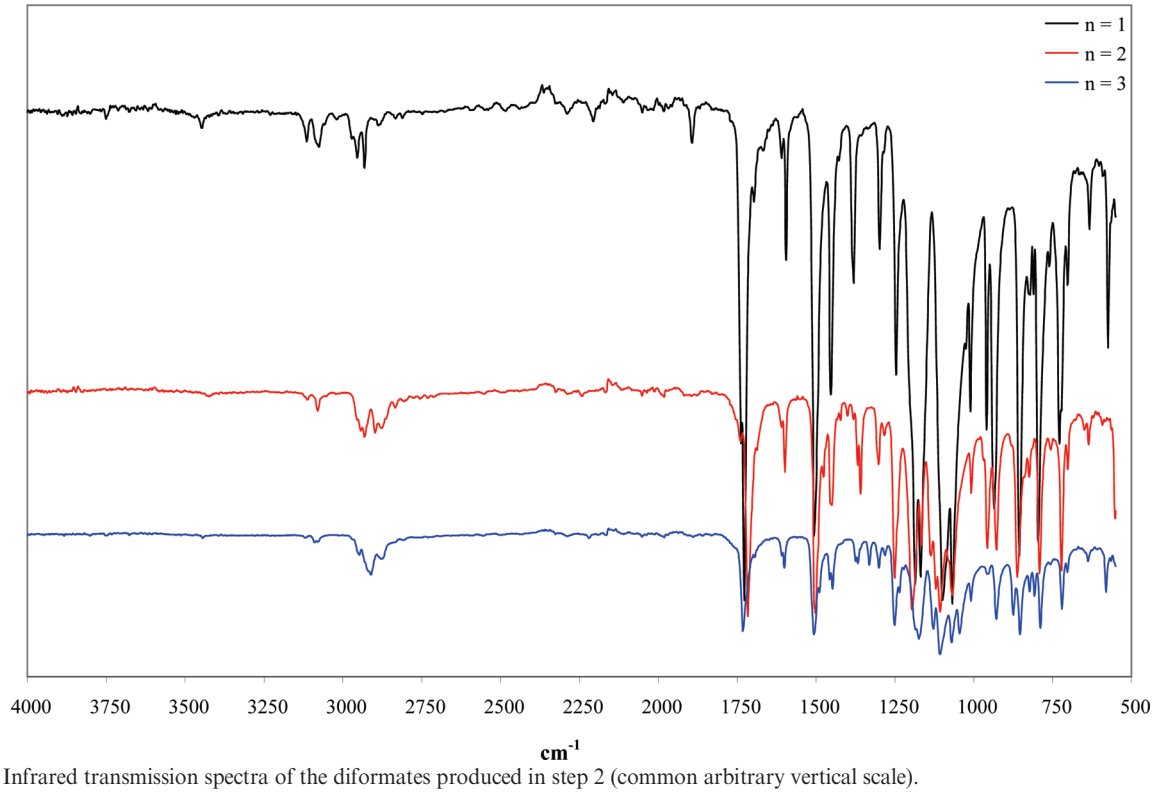

Figure 3. Infrared transmission spectra of the diformates produced in step 2 (common arbitrary vertical scale).

The infrared spectra for the products of the third step are shown in Figure 5 and reveal that the formate group has now been replaced, and this is most clearly evident from the presence of bands due to the terminal hydroxyl groups, which appear in the spectra at ~3340 cm^{-1}, and the absence of the carbonyl groups (that were previously visible at 1600−1700 cm^{-1}). The group assignments are given in Table 4.

The ^1H NMR spectrum for the diphenol (**3c**) is shown in Figure 6; having removed the effects from any carbonyl groups, only the electronegativity of the oxygen atoms present result in upfield shifts of the ring protons from 7.08 to 7.05 ppm to 6.82 to 6.69 ppm and from 6.97 to 6.94 ppm to 6.72 to 6.69 ppm. From the spectral analysis, it is evident that the cleavage of the protecting group to form terminal hydroxyl groups has been successful in producing clean materials without breaking the alkylene ether backbone. This also can be said because of the downfield position of the ethyl protons and no other fragments appear in the spectrum. One might have anticipated that the presence of hydroxyl shifts should provide useful diagnostic evidence, but whereas the hydroxyl protons are present in materials (as evidenced by the IR spectra), they are obscured by the broad shift from CD_3OD used as NMR solvent (ca. 4.88 ppm).

The final step of the scheme involves the cyanation of the diphenols to produce the desired monomers, and the FT-IR spectra in Figure 7 show that the hydroxyl group is no longer evident, accompanied by the presence of the characteristic O−C≡N stretching bands at ca. 2270 cm^{-1}. It is well known that the O−C≡N stretching bands may appear as two or more fully or partially resolved bands, although the origin of this splitting is not currently well understood,[9] but the influence of steric hindrance and crystal packing will have some influence. Therefore, the O−C≡N stretching band for **4a** appears to be split into two fully resolved bands, whereas **4b** has two fully resolved bands with a shoulder on the band appearing at 2285 cm^{-1}. Three full resolved bands are observed for **4c**, suggesting a greater

Table 3. FT-IR Assignments for the Diformates from Step 2

	compounds/observed bands (cm^{-1})		
assignment	**2a**	**2b**	**2c**
Ar−H stretch	3075	3079	3089
$-CH_2-$ stretch (ethoxy)	2954−2931	2943−2833	2948−2878
C=O formate stretching	1737−1696	1739−1716	1732−1695
ring skeleton	1609−1506	1609−1502	1608−1506
aliphatic CH_2 scissor	1453−1380	1476−1449	1457−1447
Ar−O−R (asymmetric)	1246−1185	1250−1195	1251−1221
R−O−R (symmetric)	1168−1068	1166−1120	1173−1070
1,4-disubstituted benzene ring (out-of-plane bending)	821−810	824	807

Table 4. FT-IR Assignments for the Diphenols from Step 3

	compounds/observed bands (cm^{-1})		
assignment	**3a**	**3b**	**3c**
O−H stretch	3330	3353	3352
Ar−H stretch	3068−3041	3101−3038	3088−3036
$-CH_2-$ stretch (ethoxy)	2945−2876	2927−2881	2956−2879
ring skeleton	1608−1509	1609−1506	1603−1513
aliphatic CH_2 scissor	1452−1369	1456−1448	1475−1444
Ar−O−R (aryl ether)	1268−1209	1265−1210	1269−1221
R−O−R (aliphatic ether)	1172−1069	1175−1159	1175−1111
1,4-disubstituted benzene ring (out-of-plane bending)	829−815	832−819	820

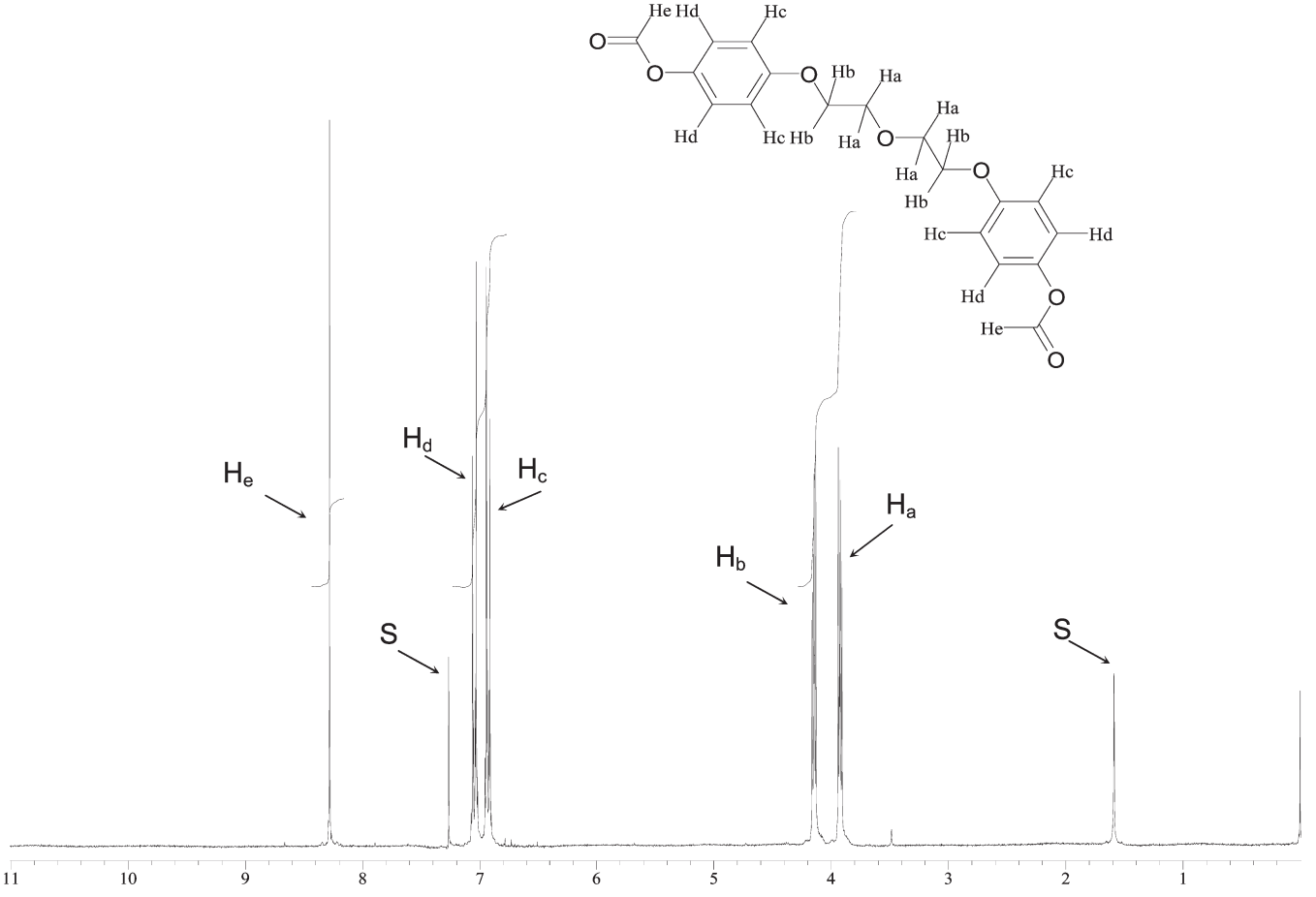

Figure 4. ^1H NMR spectrum of the diformate **2b** from step 2 (S = shifts arising from NMR solvent).

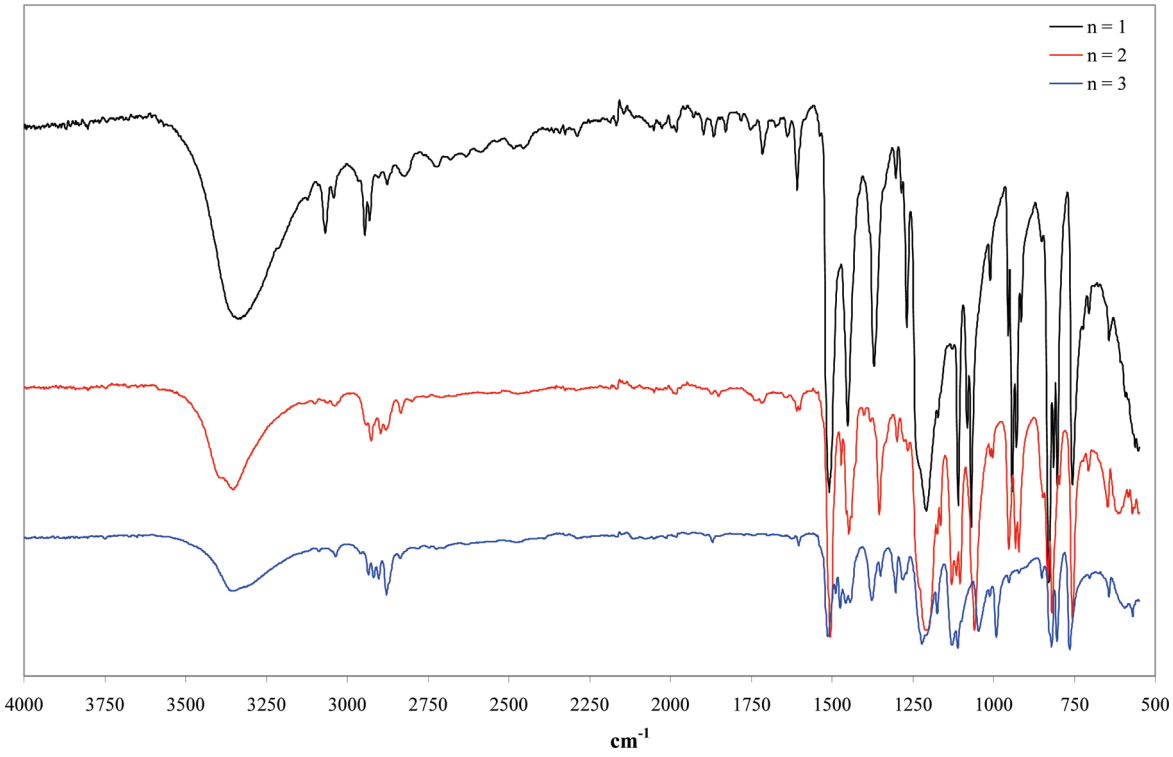

Figure 5. Infrared transmission spectra of the diphenols produced in Step 3 (common arbitrary vertical scale).

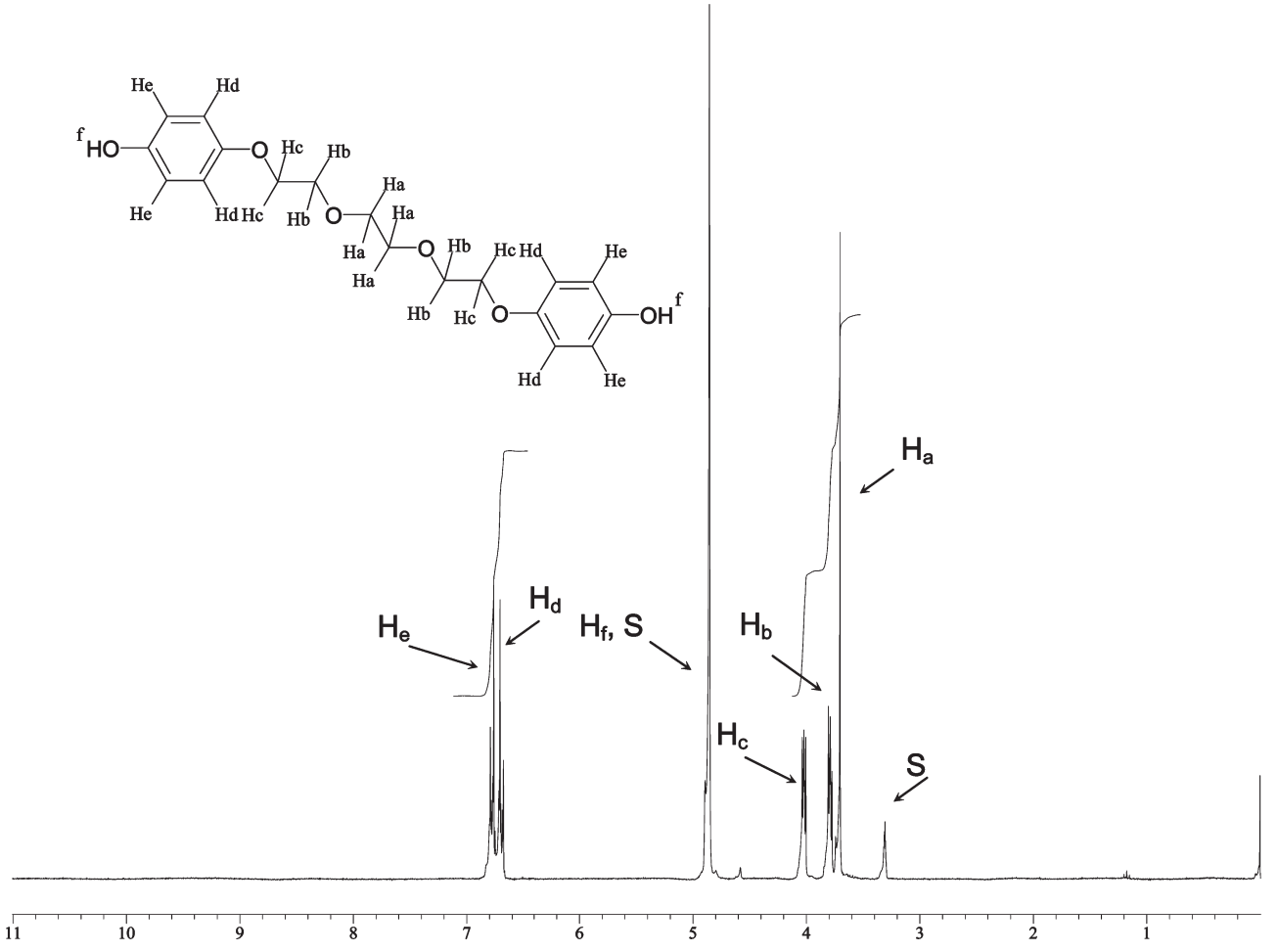

Figure 6. ^{1}H NMR spectrum of the diphenol (3c) from step 3 (S = shifts arising from NMR solvent).

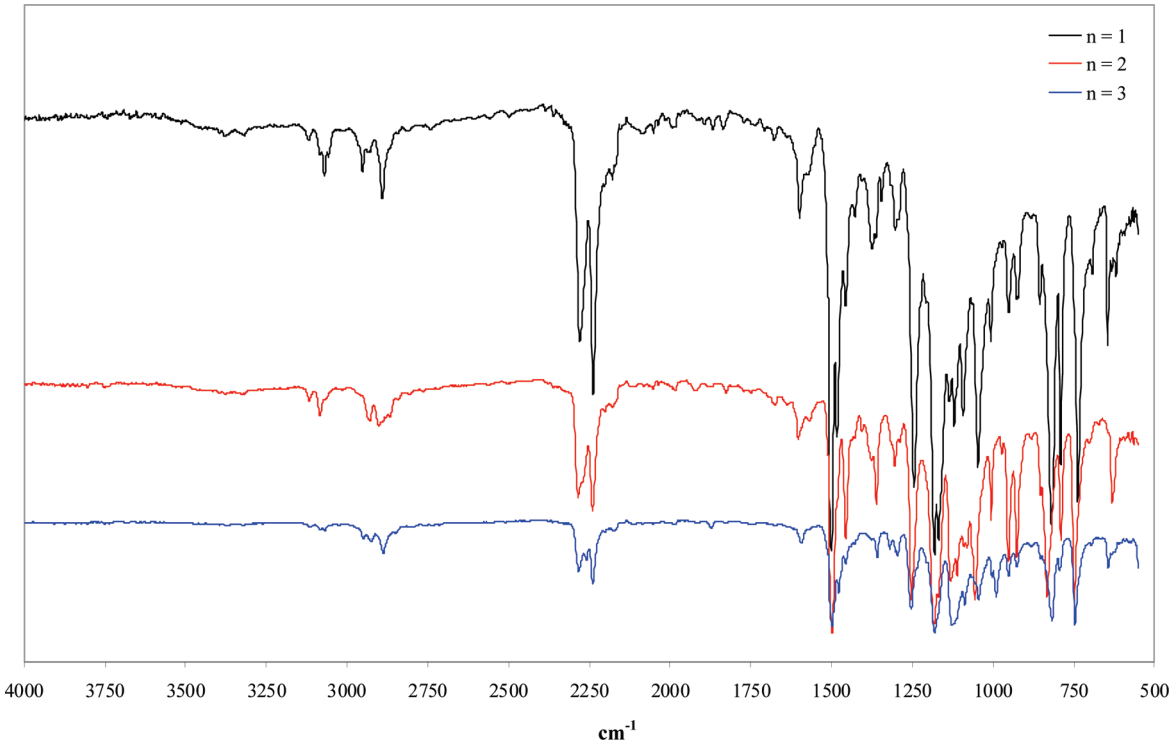

Figure 7. Infrared transmission spectra of the dicyanates produced in step 4 (common arbitrary vertical scale).

Table 5. FT-IR Assignments for the Dicyanates from Step 4

	compounds/observed bands (cm^{-1})		
assignment	**4a**	**4b**	**4c**
Ar−H stretch	3119−3070	3117−3084	3082−3069
$-CH_2-$ stretch (ethoxy)	2952−2891	2929−2902	2949−2889
O−C≡N stretching	2279−2238	2285−2240	2283−2239
ring skeleton	1598−1501	1603−1498	1592−1499
aliphatic CH_2 scissor	1456−1375	1456−1376	1456−1358
Ar−O−R (aryl ether)	1244−1181	1252−1182	1253−1180
R−O−R (aliphatic ether)	1169−1092	1170−1080	1126−1087
1,4-disubstituted benzene ring (out-of-plane bending)	819	832	817

degree of rotational freedom compared with **4a** and **4b**. The characteristic band frequencies and the corresponding assignments are shown in Table 5.

The ^{1}H NMR spectrum for the dicyanate (**4c**) produced in step 4 is shown in Figure 8. The diphenol appears to have been converted successfully to the corresponding dicyanate in reasonable purity because this ^{1}H NMR spectrum (along with the others) shows no evidence of any hydroxylated precursor remaining in the dicyanate product. The aryl protons are observed to have moved downfield as a result of the incorporation of the cyanate group, and the addition of the cyanate group serves to shift the ring protons downfield by ca. 0.3 ppm, and this is consistent with other observations in the literature.[17,18] For all of the dicyanates produced in the course of this work, the presence of the cyanate group was observed to exert a downfield shift on all of the ethyl protons in the backbone of ca. 0.1 ppm.

Examination of Blend Miscibility. The choice of the commercial dicyanate monomer AroCy B10, based on bisphenol A, as the second component in the blends was based on the extensive research literature available for direct comparison, but prior to selecting the blend compositions for analysis, an initial assessment was made of the compatibility of the individual components within the proposed blends. This assessment was based on a calculation reported by Fedors[19] (and based on the Hildebrand solubility parameter), $\delta_H = (\Delta E_v/V)^{1/2}$, where

$$\Delta E_v = \sum_i \Delta e_i \quad \text{and} \quad V = \sum_i \Delta v_i$$

(Δe_i and Δv_i are the additive atomic group contributions for the energy of vaporization and the molar volume respectively at a given temperature.) This additive method essentially produces a calculated solubility parameter, δ_H, which depends on the nature of functional groups/moieties within the monomer/polymer blend structure(s). Where the calculated values of δ_H for the two components are similar, this implies that they will be compatible. This simple method should only be taken as an initial guide to the ambient temperature compatibility of the components of the blend. It is not intended to determine the dynamics of the mixing of the components during the cure, which may be influenced by a number of factors and may lead to a complex phase diagram. On this basis, δ_H was calculated for the monomers and polymers giving the values in Table 6.

Comparing the values given in Table 6, one would expect each of the synthesized monomers to be compatible with AroCy B-10 and indeed with each other. AroCy B-30, which being a commercial prepolymer contains a larger proportion (ca. 30%) of triazine rings, should be more compatible with **4a**, because δ_H would be higher than that of AroCy B10.

Thermal Analysis of Dicyanate Monomers and Blends. The DSC thermograms arising from the analysis of uncatalyzed and catalyzed monomers are shown in Figure 9. To determine the internal self-consistency, we analyzed a catalyzed sample of 2,2-*bis*-(4-cyanatophenyl)propane (AroCy B10), for which many data have been reported, using DSC and revealed a narrow endothermic peak (peak minimum 76 °C, ΔH = 55 J/g or 15 kJ/mol cyanate). The polymerization exotherm spans 92−307 °C (peak maximum at 192 °C) with an ΔH value of 638 J/g or 178 kJ/mol cyanate; the thermal data are collected in Table 7. The uncatalyzed samples of the

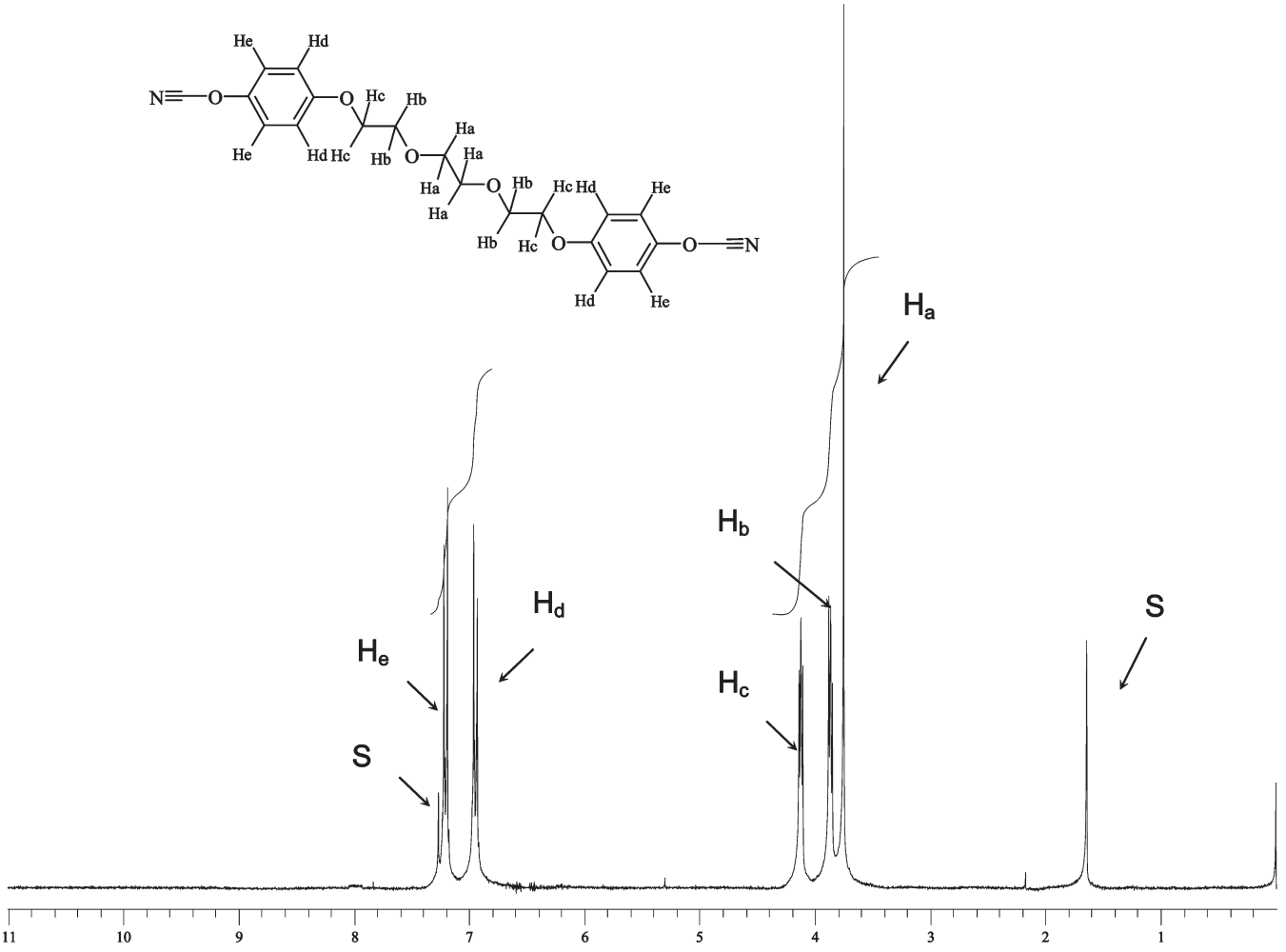

Figure 8. ^{1}H NMR spectrum of the dicyanate (**4c**) from step 4 (S = shifts arising from NMR solvent).

Table 6. Hildebrand Solubility Parameter δ_H for the Monomers and Polymers

	δ_H (MPa$^{1/2}$)	
	monomer	polymer
AroCy B10	25.20	26.69
4a	26.24	28.11
4b	25.29	26.85
4c	24.57	25.91

homologous series **4a**, **4b**, and **4c** were also analyzed in the same manner (Figure 9, Table 7).

Relatively sharp melting endotherms were observed for all three monomers: **4a**, peak minimum 125 °C and ΔH = 41 kJ/mol cyanate; **4b**, peak minimum 120 °C and ΔH = 64 kJ/mol cyanate; **4c**, peak minimum 66 °C and ΔH = 65 kJ/mol cyanate. Examination of Figure 9 also reveals broad polymerization exotherms for all uncatalyzed monomers but extremely good agreement for the total polymerization enthalpies (87 ± 2 kJ/mol cyanate), despite the variation in the temperature regime in which the process occur. As a measure of internal consistency, values reported for the thermal (i.e., "uncatalyzed") polymerization of AroCy B10 using DSC are typically 101.7,[20] 107.5,[21] 113.5,[22] 101.6,[23]and 98.7 kJ/mol^{-1} cyanate,[24] suggesting that the values here are a little depressed.

The DSC analyses of the catalyzed monomers are also presented in Figure 9 for direct comparison. It is observed that the melting endotherms occur essentially at temperatures identical to those of the uncatalyzed monomers and display similar enthalpies of fusion: **4a**, ΔH = 46 kJ/mol cyanate; **4b** ΔH = 50 kJ/mol cyanate; **4c** ΔH = 63 kJ/mol cyanate. In contrast with the melting behavior, the exothermic polymerization peaks occur at significantly lower temperatures than those of the uncatalyzed analogues and have much narrower slightly skewed profiles but tend to occur in a similar temperature regime (i.e., the peak maxima fall within 11 K (205−216 °C); these exotherms are quite symmetrical and unimodal, unlike some data that have been previously obtained[25] for catalyzed commercial monomers). The recorded polymerization enthalpies for the catalyzed monomers fall within a similar range 93 ± 9.9 kJ/mol cyanate. However, it should be noted that for the catalyzed monomers (particularly for **4b** and to a lesser extent **4a**, the fusion precedes polymerization directly, and consequently, the initial part of the polymerization exotherm is not lost. The onset limits for all catalyzed monomers were taken as the turning points (inflections in the baseline) of the affected monomers, and the decision was taken to present the catalyzed data for comparative purposes only. Even small quantities of catalyst (e.g., Al(acac)$_3$/dodecylphenol/monomer 1:25:2000) significantly lowered the peak maxima of the monomers, particularly in the case of **4a** and **4b**. The addition of the catalyst also reduced the cure onset temperatures by 50−80 K while increasing the polymerization enthalpy (Table 7).

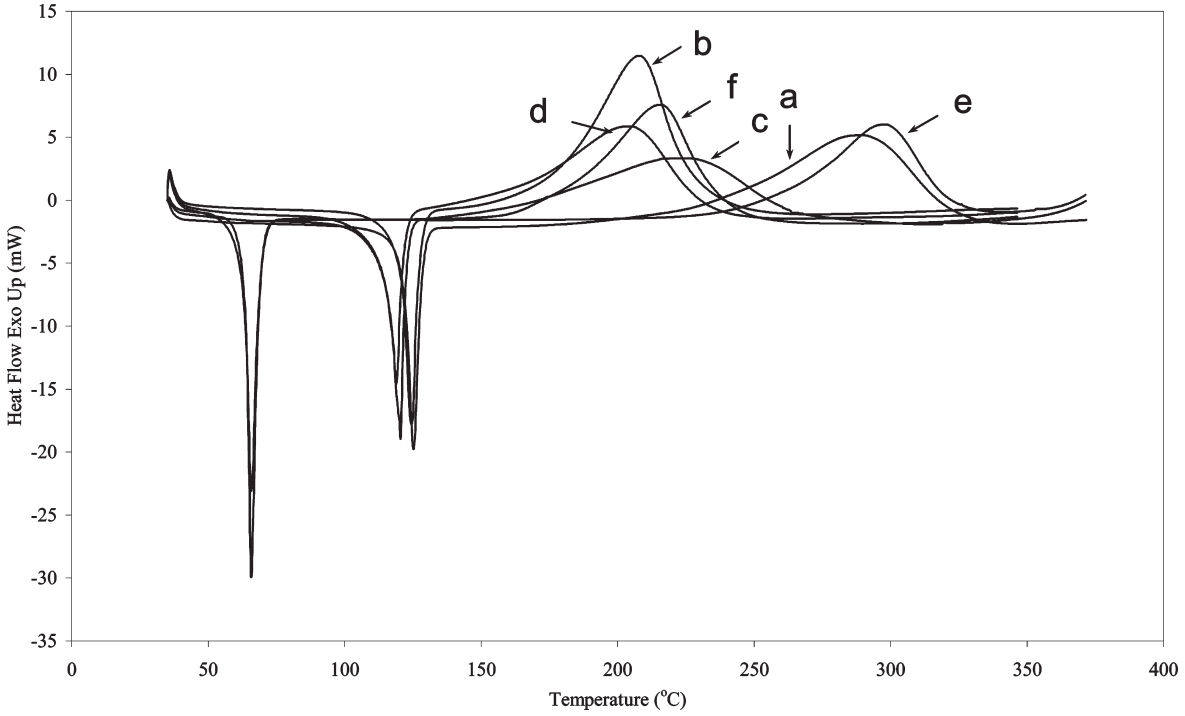

Figure 9. Composite DSC thermogram (10 K/min) of (a) uncatalyzed **4a**, (b) catalyzed **4a**, (c) uncatalyzed **4b**, (d) catalyzed **4b**, (e) uncatalyzed **4c**, and (f) catalyzed **4c**.

Table 7. Dynamic DSC Data (10 K min^{-1}) for Dicyanate Monomers and Selected Blends

				−Δ*H* polymerization	
sample	mp (°C)	cure onset (°C)	peak max (°C)	J/g	kJ/mol (OCN)
AroCy B10 (cat)	76	160	192	638	89
4a (no cat)	125	229	289	597	89
4a (cat 2000)	125	173	208	655	97
AroCy B10−**4a**	72, 106	159	194	699	99
4b (no cat)	121	151	224	516	88
4b (cat 2000)	119	156	205	483	82
AroCy B10−**4b**	73, 85	167	199	619	89
4c (no cat)	66	258	298	442	85
4c (cat 2000)	66	176	216	544	105
AroCy B10−**4c**	53, 69	172	203	616	92

It is evident from the foregoing analysis that only minimal quantities of catalyst are required to modify and improve the polymerization efficiency of the alkylene ether dicyanates. Consequently, monomers **4a**, **4b**, and **4c** were blended with catalyzed AroCy B10 in the ratio of 20:80 and analyzed using DSC (Table 7). Only one of the blends (AroCy B10−**4c**) appeared to exhibit two melting endotherms, corresponding to the AroCy B10 monomer and the alkylene ether component (Figure 10), whereas the peak minimum for the AroCy B10 melting temperature was reduced from 76 °C (as an individual monomer) to become 72, 73, and 69 °C when blended with **4a**, **4b**, and **4c**, respectively. The melting endotherms of the other blend component, the alkylene ether dicyanate, were also significantly reduced: from 125 to 106 °C for **4a**; from 121 to 85 °C for **4b**; and from 66 to 53 °C for **4c**.

The preliminary calculations of solubility (using the Hildebrand solubility parameter, δ_H) suggested that the values of AroCy B10 and **4b** for the monomers were closest in magnitude (with a difference of 0.09 MPa$^{1/2}$, Table 6) and thus should produce the most compatible blend. In contrast, and by the same token, the binary blend of AroCy B10 and **4a** should form the least compatible monomer blend (with a difference of 1.04 MPa$^{1/2}$). Therefore, the calculation suggests the following order of compatibility (where > means more soluble than): AroCy B10−**4b** > AroCy B10−**4c** > AroCy B10−**4a**, although these do not appear to be entirely borne out by the empirical observations. Significantly, where two melting endotherms were observed in a blend, only one broad polymerization exotherm was recorded in each case, suggesting some degree of compatibility in the molten state and during polymerization. Furthermore, the polymerization enthalpy is marginally greatest for the blend incorporating **4a**, although the variation in enthalpy was small (89−99 kJ mol^{-1} cyanate) for all blends analyzed and almost within the experimental variation of the technique. The values were also in very good agreement with other published analyses for dicyanate monomers.[26,7]

Thermogravimetric Analysis of the Homopolymers and Blends. AroCy B-10 (albeit using a different batch and employing different curing conditions: 180 and 230 °C/1 h) was again used as the second component in the proposed blends for this TG work, and the TGA data for the homopolymers and selected blends are given in Table 8. The TG analysis (in flowing nitrogen) of the polycyanurate of AroCy B-10 revealed an onset of thermal degradation (defined as a 5% weight loss) at 348 °C and a multistage decomposition within which few stable intermediates are formed.[27] This initial degradation step accounted for ~15% of the mass and yielded a slowly declining rate of weight loss; a second faster degradation step overlaps with the first and continues up until 530 °C. An apparently slower degradation step overlaps with the second and continues up to 800 °C, at which point the polycyanurate has not undergone complete thermal degradation and leaves a residual mass of 29%. Upon examination of the AroCy B10 degradation curve (Figure 11), it can be seen that at ~850 °C, the slope is still in very slow decline. This pattern is in agreement with other published studies for this polycyanurate.[28,15]

The possibility that the sample was not fully cured should not be excluded from the discussion, because "normal" (i.e., proscribed) cure schedules for AroCy B10 are typically more

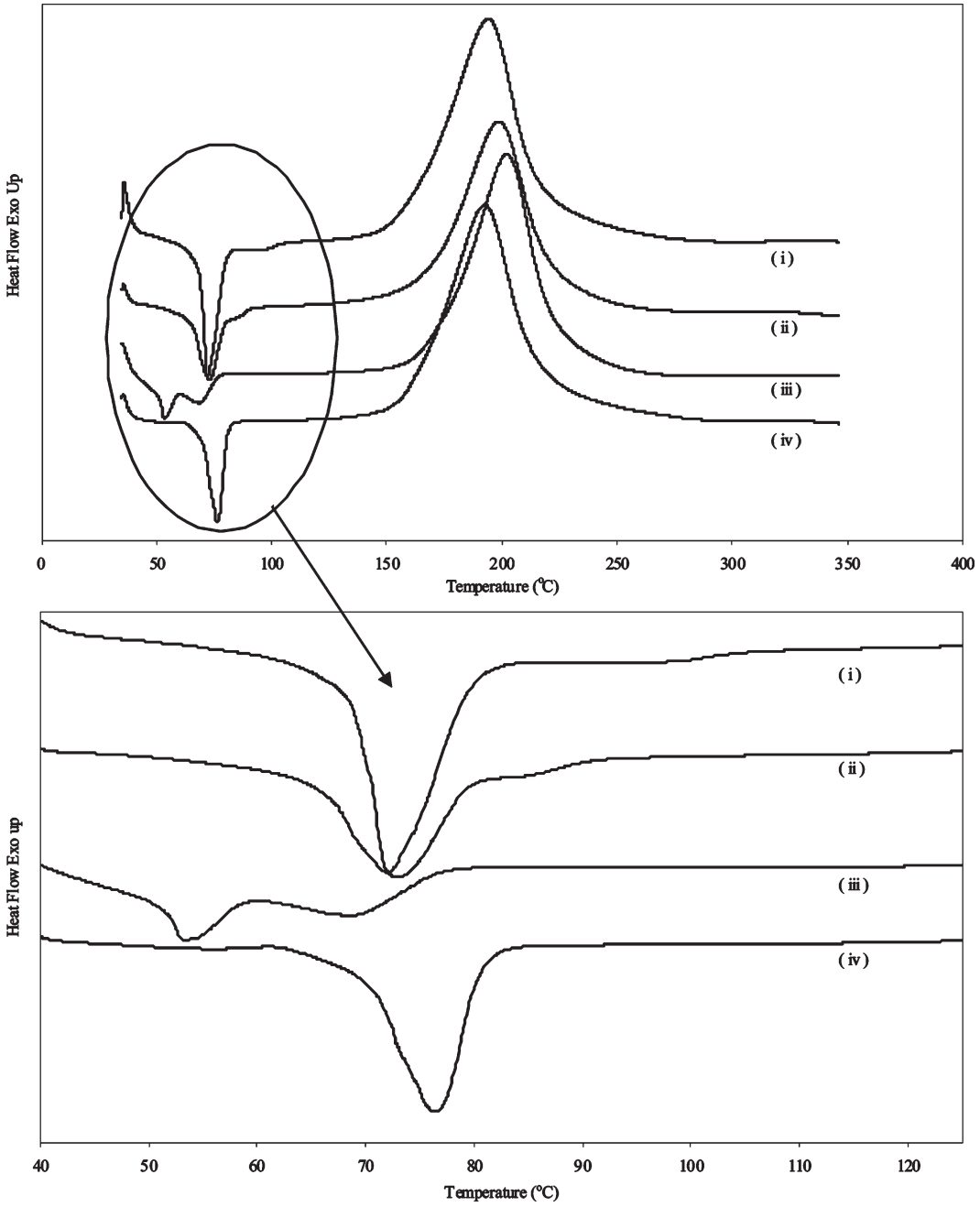

Figure 10. DSC thermograms (10 K/min) showing entire data and expansion of the melting region. (i) AroCy B10−**4a**; (ii) AroCy B10−**4b**; (iii) AroCy B10−**4c**; (iv) AroCy B10.

Table 8. TGA Data for the Thermal Degradation (In Flowing Nitrogen) of Homopolymers and Selected Blends of AroCy B10 and the Newly Reported Dicyanates

	temperature (°C) for given mass loss (%)									
sample	5%	10%	15%	20%	30%	40%	50%	60%	80%	char
AroCy B10	348	390	423	439	462	490	530	567		29%
4a	366	395	412	424	438	450	462	484		25%
4b	346	371	386	398	415	426	435	447	720	18%
4c	357	379	390	399	411	419	426	434	616	16%
AroCy B10−**4a**	356	397	424	437	456	476	517	564		29%
AroCy B10−**4b**	337	374	401	419	440	459	486	539		25%
AroCy B10−**4c**	340	375	398	412	430	446	469	517		24%

forcing depending on the eventual application and thus the T_g required.[29] Consequently, the initial degradation step might also hide some post cure process, and this was confirmed by FT-IR analysis of the cured material; showing weak O−C≡N stretching peaks at 2283 and 2220 cm^{-1} (Figure 12), the peaks are not well-defined but clearly indicate the presence of small quantities of uncured material.

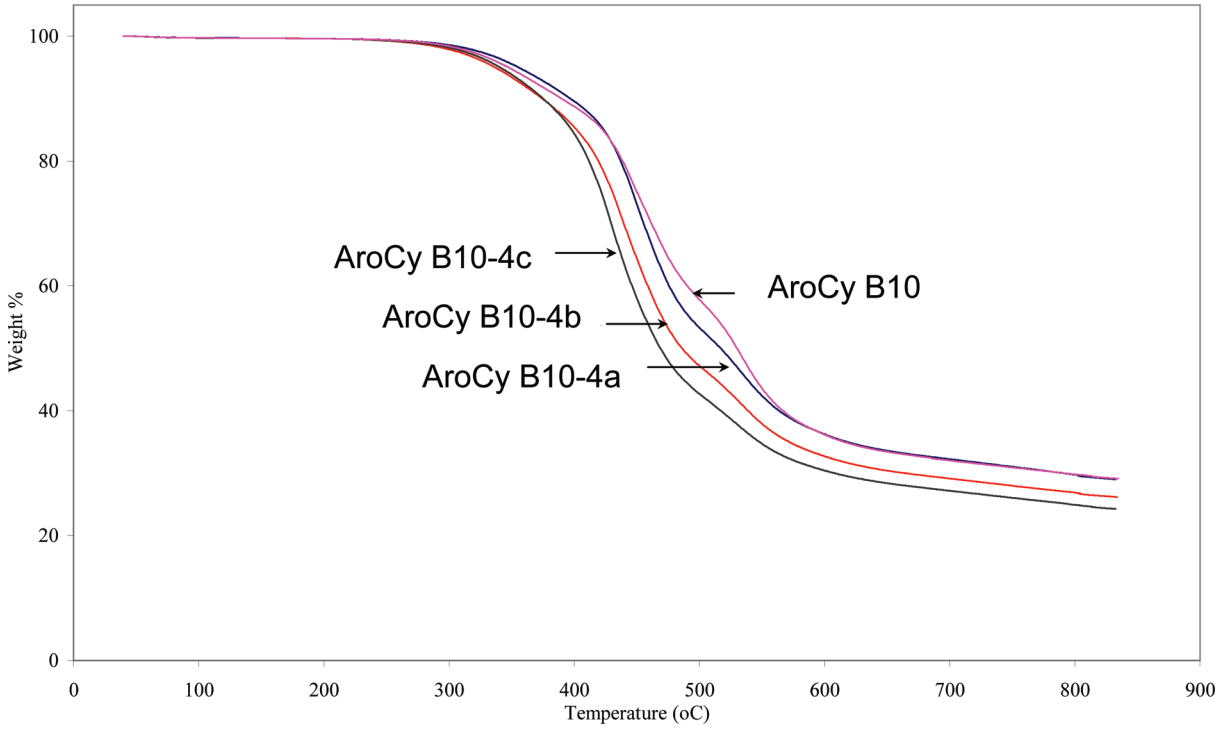

Figure 11. TG data for homopolycyanurates of AroCy B10, **4a**, **4b**, and **4c**.

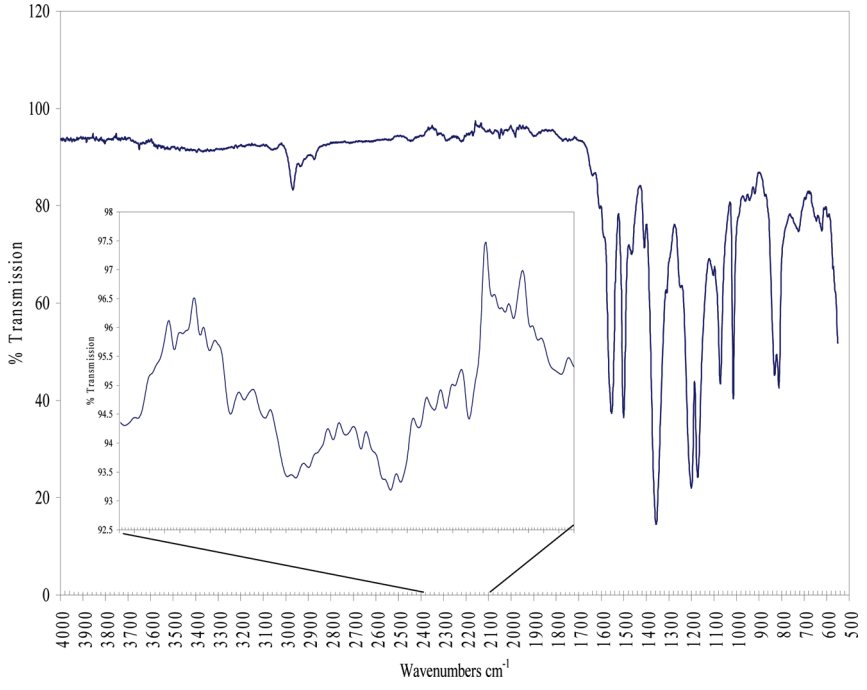

Figure 12. FT-IR (ATR) spectrum of AroCy B10 homopolymer cured at 180 and 230 °C/h (expansion of cyanate region).

FT-IR analysis of the cured alkyl ether type dicyanates did not provide conclusive evidence of the presence of any residual monomer, suggesting that the monomers were almost fully converted to their corresponding polycyanurates (Figure 12). TG analysis plots for these homopolymers showed onsets of thermal degradation (defined as a 5% weight loss) at 366 (**4a**), 346 (**4b**), and 357 °C (**4c**). All three thermograms have similar patterns of decomposition to the AroCy B10 homopolymer,[8] but predictably, thermal stability increased with decreasing backbone chain length, leaving residual masses of 25 (**4a**), 18 (**4b**), and 16% (**4c**). A similar examination of the FTIR spectra was performed to determine the degree of cure. The expansion of the spectra in Figure 13 places the features close to the limits of discrimination for the spectral analysis, and it is difficult to determine whether cyanate bands are still present in the three blends. However, it is possible to say that if the spectra do contain residual cyanate groups, then there are fewer cyanate groups than in the preceding polymers, and **4c** < **4a** < **4b** (where < means contains fewer cyanate groups). If this assumption is correct, then the effect of the alkylene ether component on the reactivity of AroCy B10 falls in the reverse order,

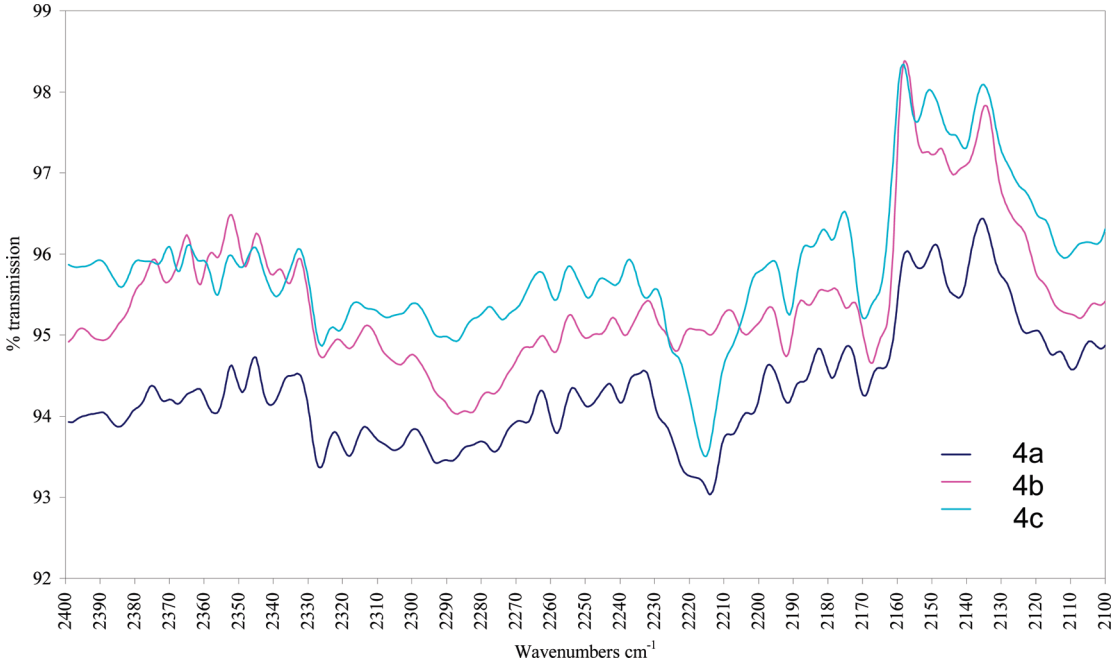

Figure 13. Partial FT-IR (ATR) spectra of newly reported dicyanate homopolymers **4a**, **4b**, and **4c** cured at 180 and 230 °C/h (showing expansion of cyanate region).

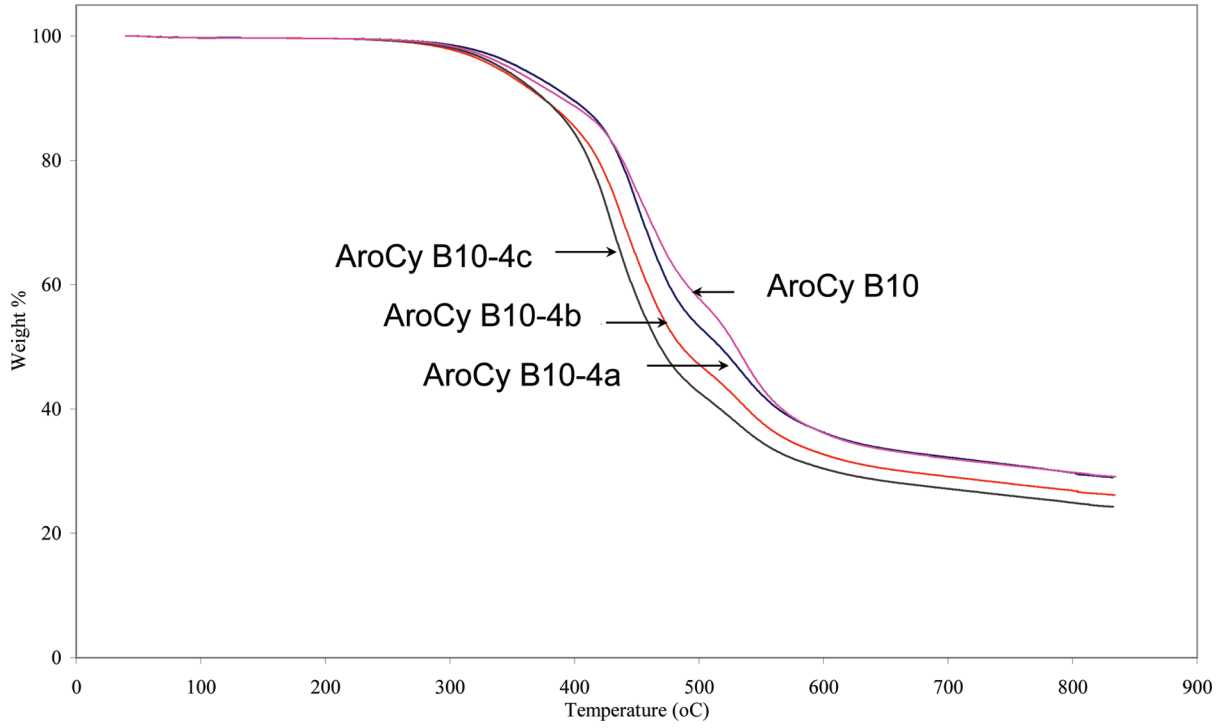

Figure 14. TGA data for homopolymer of AroCy B10 and copolymers AroCy B10−**4a**, AroCy B10−**4b**, AroCy B10−**4c**.

that is, **4c** > **4a** > **4b**, which correlates well with the order of polymerization enthalpies observed using DSC (Table 7).

The TG analyses of the blends are depicted in Figure 14 along with the homopolymer of AroCy B10. The initial onset of degradation rises in line with the suggested reactivity effect on AroCy B10 above, but the order then changes to increased stability with decreasing backbone chain length. A three-step degradation process is still observed in the blends, but this becomes less pronounced with blends containing the longer alkylene ether dicyanates; residual mass decreases with increased chain flexibility, but the effect is minimal. Therefore, the blend (AroCy B10−**4a**) appears to display a thermal stability profile that is very similar to that of the AroCy B10 homopolymer, except between 40 and 60% weight loss. The latter suggests that the less-stable alkylene ether backbone is degrading more rapidly at this point than that of the isopropyl structure.

This form of TGA plot is quite common for organic polycyanurates (i.e., indicating multistage decomposition yielding unstable intermediates). Pankratov et al. reported that the degradation products of polycyanurates consisted mainly of carbon dioxide, carbon monoxide, hydrogen,

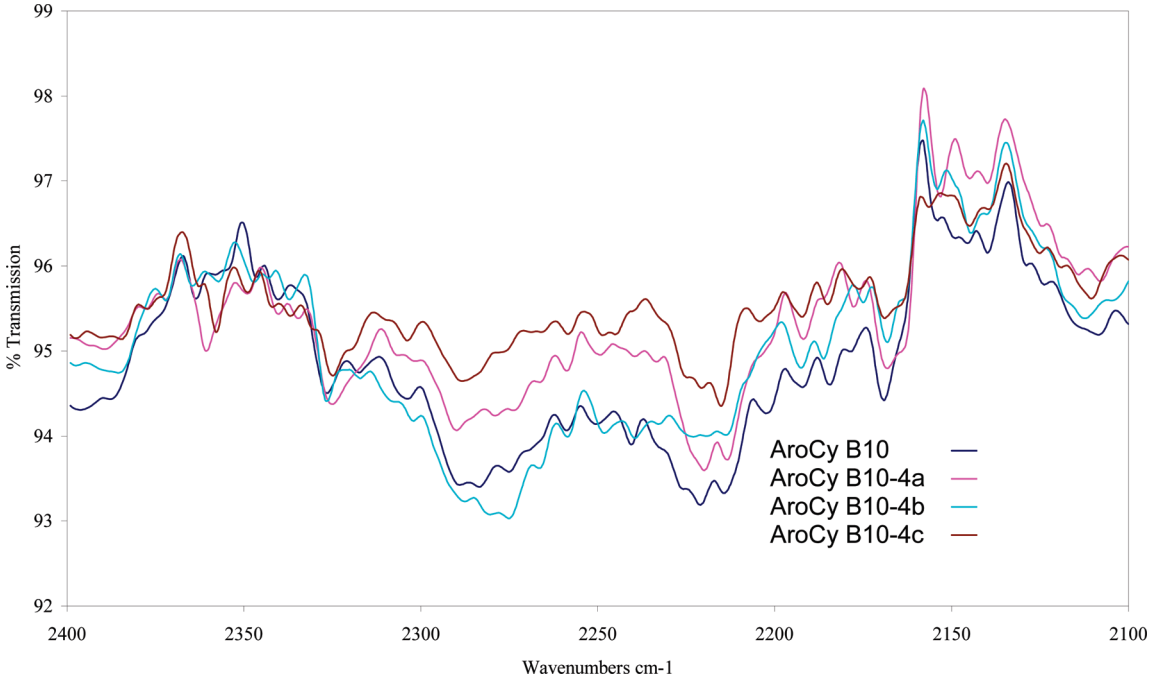

Figure 15. Partial FT-IR (ATR) spectra of AroCyB10 and the blends AroCy B10−**4a**, AroCy B10−**4b**, and AroCy B10−**4c** cured at 180 and 230 °C/h (showing expansion of cyanate region).

cyanuric acid, and its phenyl esters, phenol and bisphenols; the degradation proceeds via hydrolytic cleavage of the cyanurate prior to homo- and heterolytic decomposition of the triazine ring.[30] In more recent studies, Shimp and Ising[31] also reported that carbon dioxide arose from thermal degradation at temperatures > 200 °C, whereas Pascault et al.[32] reported that cyanic acid was a significant degradation byproduct. Using a combination of hyphenated techniques, Lyon et al.[33] found that the thermal stability for a series of common organic polycyanurates was largely independent of the chemical structure of the monomer with the major mass loss occurring at ca. 450 °C for all materials in their study. The more detailed mechanism proposed by Lyon et al. involves three consecutive processes: random scission and cross-linking of the hydrocarbon backbone between 400 and 450 °C with negligible mass loss; decyclization of the triazine ring between 450 and 500 °C, with the liberation of low-molecular-weight volatile compounds (some of which have already been mentioned in connection with the other published studies) and the formation of a primary solid residue; and decomposition of the primary residue between 500 and 750 °C.

The blends reported here are marginally less thermally stable than a previous examination of blends of aromatic dicyanate monomers,[31] but this reflects the higher aliphatic content in the present materials, which predominates in the first step of the mechanism proposed by Lyon et al. In that previous article, the initial degradation step that was observed for cured AroCy B10 might also have hidden some post cure process, and this was confirmed by FT-IR analysis of the cured material. Weak O−C≡N stretching peaks at 2283 and 2220 cm^{-1} were observed (Figure 15); although the peaks were not well-defined, they did clearly indicate the presence of small quantities of uncured material.

FT-IR spectral analysis (albeit in transmission) shows very weak cyanate bands amounting to perhaps ca. 2 to 3% under the cure conditions employed. The aforementioned FT-IR analysis of the cured alkyl-ether-type dicyanates suggested that the homopolymers had undergone a marginally more advanced cure with still weaker bands attributable to residual monomer under these cure conditions. The blends containing AroCy B10 and the alkylene ether cyanates behaved in a similar fashion under these cure conditions. It is unwise to make too many observations of transmission data, which are by their very nature not truly quantitative, with very weak signals, which approach the limits of the signal/noise ratio of the spectrometer. However, the groups giving rise to the bands should have similar polarities, so a broad comparison might be made. It does appear that there are possibly fewer cyanate groups remaining (i.e., leading to a greater degree of conversion) in the polycyanurate blend containing **4b**, falling in the order **4c** > **4a** > **4b**, which correlates well with the order of polymerization enthalpies observed in the DSC analysis previously presented.

Dynamic Mechanical Thermal Analysis of the Homopolymers and Selected Blends. The thermograms arising from the DMTA of the catalyzed polymers are shown in Figure 16. Once again, a catalyzed sample of AroCy B10 was analyzed using DMTA and revealed a glass-transition temperature, T_g (the α transition) of 277 °C (determined from the maximum value of the loss tangent, tan δ). Other low-temperature transitions (β and γ) were also present; the thermal data are collected in Table 9. The storage modulus falls noticeably (E' = 2.14 GPa at 25 °C and E' = 1.70 GPa at 150 °C) prior to the glass transition. The T_g values of the homopolymers of **4a**, **4b**, and **4c** were also determined from the peak maxima of the tan δ data and the values of 221 °C (**4a**), 139 °C (**4b**), and 121 °C (**4c**) fall in the expected order of T_g decreasing as the backbone chain length, and hence flexibility is increased. Examination of the storage moduli revealed more mixed results: **4a**), E' = 1.77 GPa at 25 °C, 1.60 GPa at 50 °C, and 1.13 GPa at 150 °C; **4b**, E' = 2.67 GPa at 25 °C, 2.38 GPa at 50 °C, and 1.81 GPa at 100 °C; **4c**, E' = 1.80 GPa at 25 °C and 1.62 GPa at 50 °C.

Direct (quantitiative) comparison of the three backbones is difficult because of the nature of the onset temperatures of glassy to rubbery states. However, when considering the

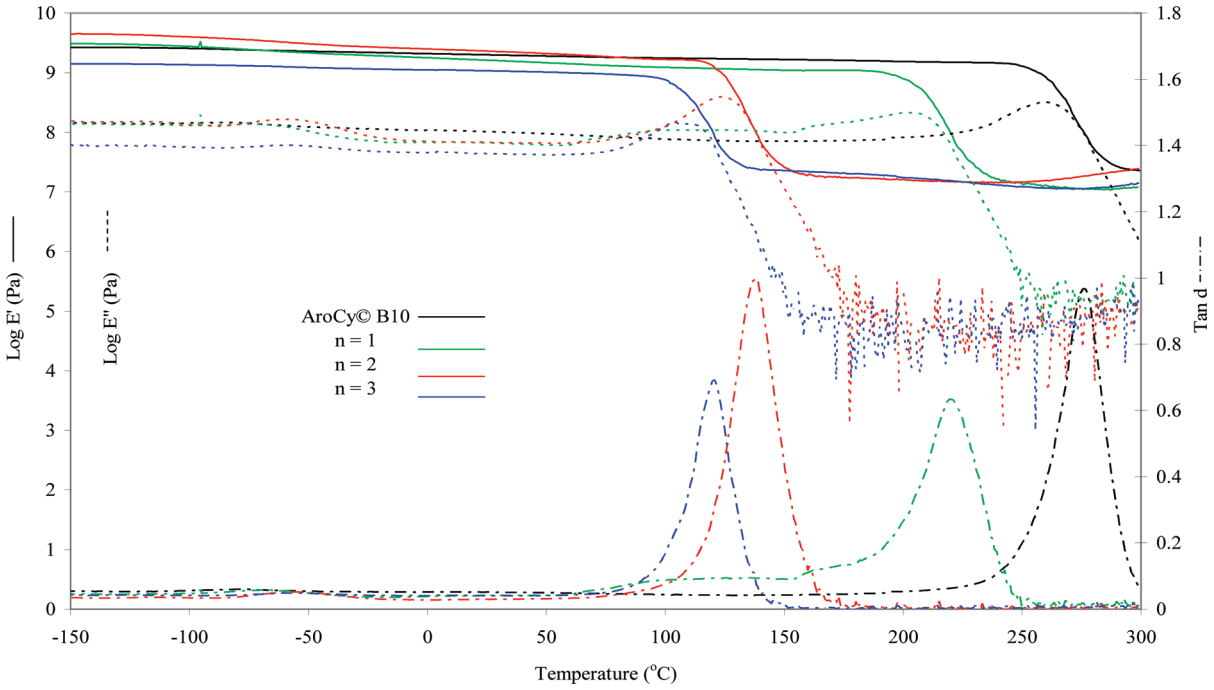

Figure 16. DMTA data for homopolymers of AroCy B10 and **4a**, **4b**, and **4c**.

Table 9. DMTA Data for Poly(2,2-*bis*(4-cyanatophenyl)propane) the Newly Reported Dicyanates and Selected Binary Blends

samples	α transition (°C)	β transition (°C)[a]	γ transition (°C)
AroCy B10	277	30	−80
4a	221	24	−68
4b	139	−55	−115
4c	121	−55	−115
AroCy B10−**4a**	275	35	−82
AroCy B10−**4b**	241	20	−77
AroCy B10−**4c**	247	35	−63

[a] With the exception of **4b**, this transition is ill-defined and very broad.

storage modulus, a general trend is observed; that is, **4b** > AroCy B10 ≫ **4c** > **4a**, where the **4b** storage modulus is significantly higher than that of AroCy B10 by ca. 0.4 GPa and ca. 0.8 GPa higher than **4c** and **4a**. This observation is contrary to the corresponding T_g values for the homopolymers, for which the order **4a** > **4b** > **4c** is observed (i.e., directly reflecting the length of the backbone and cross-link density).

The relative heights of the tan δ peaks suggest that **4b** is a less-brittle material, as evident of the high storage modulus of 2.10 GPa at 80 °C, whereas **4a** is perhaps the most brittle, which is consistent with the higher cross-link density generated in the polymer.

The newly prepared dicyanates **4a**, **4b**, and **4c** were then added to AroCyB10, each at a ratio of 20:80 wt % and cured to produce what appear to be homogeneous copolymers (as evidenced by single-step transitions in the loss modulus data and single α transition peaks for each copolymer (Figure 17)). From an examination of the DMTA data, it appears that storage modulus (E') of AroCy B10 is affected to differing extents by the addition of the alkylene ether dicyanates (**AroCy B10−4a**), E' = 1.02 GPa at 25 °C, 0.98 GPa at 50 °C, and 0.88 GPa at 200 °C; (**AroCy B10−4b**), E' = 2.01 GPa at 25 °C, 1.92 GPa at 50 °C, and 1.73 GPa at 200 °C; (**AroCy B10−4c**), E' = 1.47 GPa at 25 °C, 1.43 GPa at 50 °C, and 1.31 GPa at 200 °C.

Although the storage moduli at 25 °C for the binary blends are significantly lower than those of the respective homopolymers,[11] the reduction in E' over the temperature range 25−200 °C has significantly improved compared with AroCy B10 (which loses some 0.56 GPa over this range). For example, the introduction of **4b** appears to improve this by a factor of ca. 2, whereas **4a** and **4c** improve it by a factor of ca. 4. Considering that the T_g values of the homopolymers are relatively low, 139 (**4b**) and 121 °C (**4c**), respectively,[11] the addition of the second component does not apparently affect the T_g of AroCy B10 significantly when blended to form a copolymer (at this level of incorporation), giving values of 241 and 247 °C, respectively. (See Table 9.) Examination of the shape of the tan δ peak is also quite informative, with the taller peak shapes (and greater half peak width) being indicative of superior damping properties. Within this study, the blend containing the chain of intermediate length, AroCy B10−**4b**, was apparently significantly tougher than the next pair, AroCy B10 and AroCy B10−**4a** (which were apparently almost identical in this characteristic), and perhaps surprisingly significantly better than AroCy B10−**4c**, bearing the most flexible chain. This appears to be counterintuitive, but perhaps with increasing chain length, the opportunities for intermolecular association (via a combination of dispersion forces and dipole−dipole interactions) actually begin to increase following an initial reduction (cf. the variation in T_g that is observed with (*n*-alkyl) pendant methacrylate polymers), where an increase in the size and bulkiness of the pendant groups leads to an initial reduction in the T_g of the material because of the increased free volume generated between polymer chains,[34] allowing for freer rotation of the polymer chains, lowering the T_g, and thereby reducing the amount of energy required for the T_g to be reached. Beyond this, when the number of methylene groups pendant on the polymer chain exceeds eight, it has been observed that the T_g values of the materials increase once more. This is due to entanglement of the chains leading to crystallization. This aspect is currently receiving further attention as we apply tried and tested molecular simulation techniques[35] to investigate this phenomenon in these dicyanates.

Thermomechanical Analysis of Selected Blends. The binary blends of AroCy B-10 and the newly prepared dicyanates

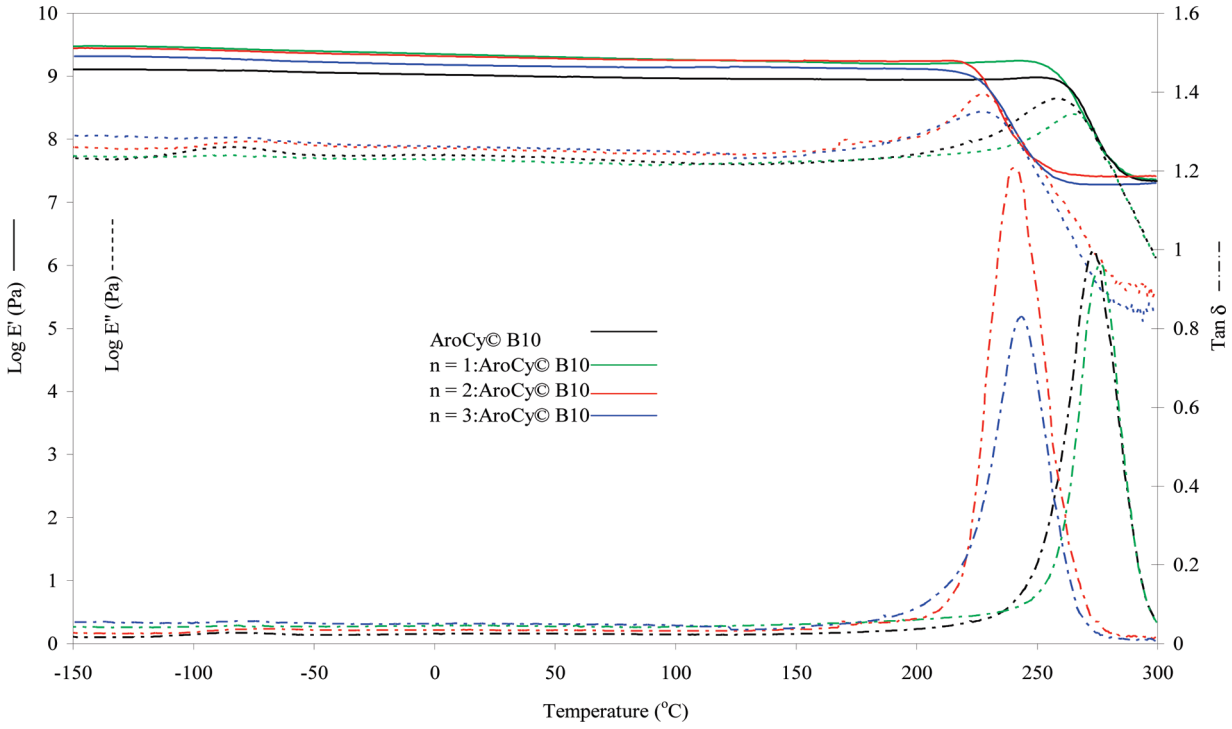

Figure 17. DMTA data for homopolymer of AroCy B10 and selected blends AroCy B10−**4a**, $n = 1$; AroCy B10−**4b**, $n = 2$; AroCy B10−**4c**, $n = 3$.

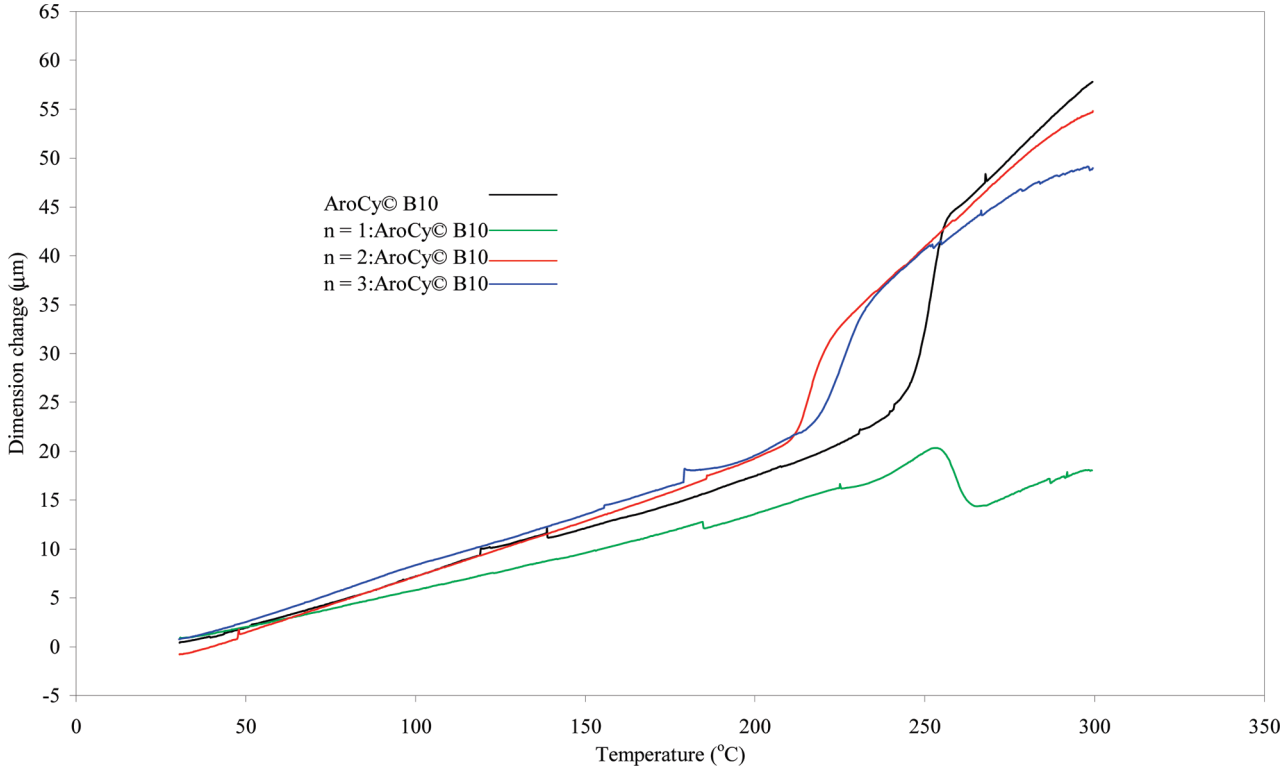

Figure 18. TMA data for homopolymer of AroCy B10 and selected blends AroCy B10−**4a**, $n = 1$; AroCy B10−**4b**, $n = 2$; AroCy B10−**4c**, $n = 3$.

were analyzed using TMA, and reasonably good agreement was found between this technique and DMTA (e.g., the T_g for AroCy B-10 was determined to be 279 °C using DSC (10 K min^{-1}) and 246−256 °C using TMA, with a value of 87 ppm/°C between 40 and 200 °C). However, it is well-known that the tan δ measurement yields an optimistic value for T_g, and if one determines this value from the peak of the loss modulus (or midpoint of the drop in storage modulus) of our data, then a value of 250−255 °C is obtained. The CTE value determined here compares favorably with that reported for commercial samples of AroCy B10, for example, 64 ppm/°C between 40 and 200 °C,[36] although this parameter is influenced strongly by the degree of conversion and cross-link density, and this is often not mentioned in commercial literature. The analysis of the binary blends using TMA yielded data (Figure 18) in good agreement with the DMTA

Table 10. TMA Data for Homopolymer of AroCy B10 and Selected Blends

	T_g (°C)	CTE (ppm/°C)
AroCy B10	246−256	87
AroCy B10−**4a**	255−263	75
AroCy B10−**4b**	212−221	91
AroCy B10−**4c**	220−236	95

measurements previously recorded with the same apparent slight reversal in order of T_g: AroCy B10−**4a** > AroCy B10−**4c** > AroCy B10−**4b**. Of the blends examined here, the one incorporating the shortest alkylene backbone AroCy B10−**4a** showed the greatest T_g with the lowest value of CTE (Table 10) and would have yielded the best high-temperature candidate with the lowest expansion to fulfill the initial brief.

Conclusions

It is evident from the data and analysis presented in this article that the method used in this study was more efficient and less demanding than that of Jiang et al.,[12] who prepared the dialdehyde (**1a**) under more forcing conditions (i.e., dibromoethane and 4-hydroxybenzaldehyde with LiH as the reducing agent at −78 °C in EtOH) over a longer time scale (>2.5 days) in poorer yield (63%). The same is true of the method employed to produce **3a**, which was previously synthesized by Guilani et al.[14] using sodium metal dissolved in EtOH and refluxed overnight to yield 40%. In contrast, in the current work, each individual step for all three backbone types produced excellent yields of >70%, thus giving an overall reaction yield for all four steps of 42% for **4a**, 44% for **4b**, and 50% for **4c**. The main difficulty encountered in the preparation represented in Scheme 1 was, in all cases, step 2. The addition of MCPBA produced a strongly exothermic reaction, although the heat evolved decreased as the backbone chain length progressively increased, and this was accompanied by an increase in the reaction time. Future work with this structure requires some caution to be employed when carrying out this step, and some investigation will be made as to whether the reaction might not be usefully carried out at reduced temperature rather than at room temperature.

A variety of analytical results are presented to show that the selected binary blends incorporating 20 wt % of the newly prepared dicyanate monomers yield polycyanurates with reactivities that are comparable to those of the commercial dicyanate AroCy B10. The thermal stabilities (in terms of the onset of degradation, char yield, etc.) of the polymer blends are also similar to those of AroCy B10 and apparently display the same degradation mechanism. Measurements made of the dynamic mechanical and thermomechanical properties reveal that all blends produce thermoset polymers with glass-transition temperatures that are of similar magnitude to AroCy B10 and, in the case of the blend AroCy B10−**4a** (containing the shortest alkylene ether), essentially the same value. At the same time, this blend also yields a polymer with a significantly lower CTE than the commercial homopolymer. A study is currently underway to examine binary blends involving the same constituents to determine the optimum composition to yield the best combination of properties, and a study of fracture mechanics will then be undertaken.

Acknowledgment. We thank Hitachi Chemical Co. Ltd. for funding this work in the form of a studentship (P.K.). At the University of Surrey, we thank Ms. Nicola Walker for performing the elemental analyses and Mr. James P. Bloxsidge for obtaining some of the NMR spectra.

References and Notes

(1) Weirauch, K. K. *Proceedings of the IPC Sept. 1975 Meeting*, Chicago, IL, 1975; paper no. TP-066
(2) Speak, S. C.; Sitt, H.; Fuse, R. H. *36th Int. SAMPE Symp.* **1991**, *36*, 336.
(3) Sweetman, E. *Proceedings of the 1st International Conference on Multichip Modules* (sponsored by ISHM and IEPS), Denver, CO, 1992; p 401.
(4) Hamerton, I. Chapter 1: Introduction to Cyanate Ester Resins. In *Chemistry and Technology of Cyanate Esters*; Hamerton, I., Ed.; Blackie: New York, 1994; pp 1−6.
(5) Shimp, D. A.; Christenson, J. R.; Ising, S. J. *34th Int. SAMPE Symp. Exhib.* **1989**, *34*, 222.
(6) Almen, G. R.; Mackenzie, P. D.; Malhotra, V.; McGrail, P.T. *20th Int. SAMPE Tech. Conf.* **1988**, *20*, 46.
(7) Snow, A. W. Chapter 2: Cyanate Ester Monomers. In *Chemistry and Technology of Cyanate Esters*; Hamerton, I., Ed.; Blackie: Glasgow, 1994; pp 48−50.
(8) Grigat, E.; Pütter, R. German Patent 1,195,764, **1963**.
(9) Grigat, E.; Pütter, R. *Chem. Ber.* **1964**, *97*, 3012.
(10) Klewpatinond, P. Ph.D. Thesis, University of Surrey, **2005**.
(11) Bhatt, M. V.; Kulkarni, S. U. *Synthesis* **1983**, 249.
(12) Takeda, S.; Akiyama, H.; Kakiuchi, H. *J. Appl. Polym. Sci.* **1988**, *35*, 1341.
(13) Jiang, J.; Compere, E. L.Jr. *Synth. Commun.* **1998**, *28*, 1041.
(14) Simion, C.; Simion, A.; Mitoma, Y.; Nagashima, S.; Kawaji, T.; Hashimoto, I.; Tashiro, M. *Heterocycles* **2000**, *53*, 2459.
(15) Guilani, B.; Rasco, M. L.; Hermann, C. F. K.; Gibson, H. W. *J. Heterocyclic Chem.* **1990**, *27*, 1007.
(16) Nagvekar, D. S.; Gibson, H. W. *OPPI Briefs* **1997**, *29*, 234.
(17) Barton, J. M.; Hamerton, I.; Jones, J. R. *Polym. Int.* **1992**, *29*, 145.
(18) Chaplin, A.; Hamerton, I.; Howlin, B. J.; Barton, J. M. *Macromolecules* **1994**, *27*, 4927.
(19) Fedors, R. F. *Polym. Eng. Sci.* **1974**, *14*, 147.
(20) Shimp, D. A. *ACS PMSE Prepr.* **1986**, *54*, 107.
(21) Barton, J. M.; Greenfield, D. C. L.; Hamerton, I.; Jones, J. R. *Polym. Bull.* **1991**, *25*, 475.
(22) Bauer, M.; Bauer, J.; Garske, B. *Acta Polym.* **1986**, *37*, 604.
(23) Osei-Owusu, A.; Martin, G. C.; Gotro, J. *Polym. Eng. Sci.* **1991**, *31*, 1604.
(24) Georjon, O.; Galy, J.; Pascault, J.-P. *J. Appl. Polym. Sci.* **1993**, *49*, 1441.
(25) Barton, J. M.; Hamerton, I.; Jones, J. R. *Polym. Int.* **1993**, *31*, 95.
(26) Hamerton, I.; Emsley, A. M. E.; Howlin, B. J.; Klewpatinond, P.; Takeda, S. *Polymer* **2003**, *44*, 4839.
(27) Brown, M. E. Interpretation of TG and DTG Curves. In *Introduction to Thermal Analysis: Techniques and Applications*; Chapman & Hall: London, 1988; p 18.
(28) Hamerton, I.; Emsley, A. M.; Howlin, B. J.; Klewpatinond, P.; Takeda, S. *Polymer* **2004**, *45*, 2193.
(29) Ising, S. J.; Shimp, D. A. *34th Int. SAMPE Symp.* **1989**, *34*, 1326.
(30) Korshak, V. V.; Gribkova, P. N.; Dmitrienko, A. V.; Puchin, A. G.; Pankratov, V. A.; Vinogradova, S. V. *Vysokomol. Soedin.* **1974**, *A16*, 15.(cited in Pankratov, V. A.; Vinogradova, S. V.; Korshak, V. V. *Russ. Chem. Rev.*, **1977**, *46*, 278).
(31) Shimp, D. A.; Ising, S. J. *Proc. ACS Div. Polym. Mater. Sci. Eng.* **1991**, *66*, 504.
(32) Mirco, V.; Méchin, F.; Pascault, J.-P. *Proc. ACS Div. Polym. Mater. Sci. Eng.* **1994**, *71*, 688.
(33) Ramirez, M. L.; Walters, R.; Savitski, E. P.; Lyon, R. E. *Thermal Decomposition of Cyanate Ester Resins*; Final Report DOT/FAA/AR-01/32; U.S. Department of Transportation, Federal Aviation Administration: Washington, D.C., 2001.
(34) Howard, C. *Trends Polym. Sci.* **1995**, *1*, 336.
(35) Hamerton, I.; Howlin, B. J.; Klewpatinond, P.; Takeda, S. *Polymer* **2002**, *43*, 4599.
(36) Hamerton, I. Chapter 7: Properties of Unreinforced Cyanate Ester Matrix Resins. In *Chemistry and Technology of Cyanate Esters*; Hamerton, I., Ed.; Blackie: Glasgow, 1994; p 209.